

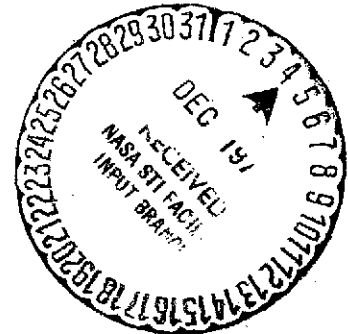
FINAL TECHNICAL REPORT  
AAFE MAN-MADE NOISE EXPERIMENT PROJECT

VOLUME III  
APPENDICES

JUNE 1974

(NASA-CR-132511) AAFE MAN-MADE NOISE EXPERIMENT PROJECT. VOLUME 3: APPENDICES Final Technical Report (National Scientific Labs., Inc.) 107 p HC \$5.25	N75-12170    Unclas CSCL 17B G3/32 03490
--	---

Prepared under  
Contract NAS 1-11465



Prepared for  
National Aeronautics and Space Administration  
Langley Research Center  
Hampton, Virginia 23365

**National Scientific Laboratories, Inc.**  
**Westgate Research Park, McLean, Virginia 22101**

A Subsidiary of Systematics General Corporation

FINAL TECHNICAL REPORT  
AAFE MAN-MADE NOISE EXPERIMENT PROJECT

VOLUME III  
APPENDICES

JUNE 1974

Prepared under  
Contract NAS 1-11465

Prepared for  
National Aeronautics and Space Administration  
Langley Research Center  
Hampton, Virginia 23365

**National Scientific Laboratories, Inc.**  
**Westgate Research Park, McLean, Virginia 22101**

---

A Subsidiary of Systematics General Corporation

APPENDIX A  
LAUNCH AND ORBIT

TABLE OF CONTENTS

<u>APPENDIX</u>	<u>PAGE</u>
A LAUNCH AND ORBIT-----	A-1
B EXPERIMENT MANAGEMENT-----	B-1
C RECEIVER SCANNING CONSIDERATIONS-----	C-1
D DATA HANDLING-----	D-1
E THRESHOLD MEASUREMENTS-----	E-1

## A. LAUNCH AND ORBIT

### A.1 General

The tentative launch vehicle selected as optimum for the experiment payload was a Scout D. A number of preliminary calculations have been made based on the use of this vehicle for the orbit of choice. The assessment of other vehicles is continuing, however, because the ability of the Scout D or Scout E to provide the necessary performance now appears, at best, marginal. There is a considerable likelihood that the uprated Scout mentioned in the following paragraphs will be able to provide required performance and will be available well within the time frame of the orbited Man-Made Noise Experiment.

Another possible approach to the problem of launch may be to use two satellites, with two launch vehicles of the Scout class in circular orbits. This approach, now under consideration, would simplify a number of factors, including data reduction and analysis. Its feasibility will be determined by the relative cost of two equipped spacecraft and launches and that of a single "outfit". It is hoped that this trade-off can be developed further through acquisition of launch vehicle and launch cost data.

### A.2 Launch Vehicles

In order to assure interface compatibility between spacecraft and launch vehicle, an investigative study is underway to define payload capabilities of the following expendable launch vehicles:

- (1) Scout D

- (2) Scout E
- (3) Scout E with additional velocity package
- (4) Up-rated Scout (Higher energy propellant)
- (5) Delta 2310

A literature search as well as direct contact with Mr. J. E. McGolrick at NASA HQ. and Mr. Norm Fisher at Batelle Memorial Institute have produced the following results:

(1) Scout D

Scout D consists of 4 solid propellant non-restartable stages with launch facilities at Wallops Island, ETR (Eastern Test Range) and WTR (Western Test Range). Non-restartable staging requires complexity in burn and coast times in the two impulse maneuvers to achieve apogee, perigee and inclination. Preliminary calculations indicate that for a launch within range safety limitations, at Wallops Island, directly into desired apogee and perigee and with the fourth stage supplying the desired orbit inclination change, the payload capability is approximately 111 kg. If staging is such that azimuth safety limitations can be waived, and orbit inclination is achieved without the necessity of a plane change the payload capability would be approximately 140 kg.

(2) and (3) Scout E and Scout E with Velocity Package

Although investigation of this five stage Scout is still underway it does not appear that this up-rated Scout version will buy much in performance. A fifth stage and velocity package are cost effective if the payload weight is small (< 50-100 kg).

(The man-made noise experiment payload is anticipated at about 150-200 kg).

(4) Upated Scout

A significantly uprated version of the Scout launch vehicle is being developed which will fill in the enormous cost-performance gap between the Scout E and the Delta. Higher energy propellant is used to increase performance. Another possibility is to mate burned II upper stages with TAT (nC) boosters for an intermediate thrust between Scout and Delta. Investigation of these uprated versions is continuing.

(5) Delta

Payload capability and cost of the Delta launch vehicle are both unnecessarily high for the anticipated payload requirements of the man-made noise experiment. It may be possible, however unlikely, that the package may ride "piggyback" with another payload if a means by which the two may assume different orbits is employed.

A.3 Preliminary Launch Considerations

The vecocity requirements of non-restartable launch vehicles for achieving the desired orbit under consideration vary depending primarily upon launch azimuth. Launch sites have established range safety limitations such that stages after fuseout will fall into the ocean rather than on land. Investigation of these launch azimuth limitations indicate that at none of the available launch

sites can a  $63.4^\circ$  orbital inclination be achieved through an appropriate launch azimuth. Under certain staging conditions these launch azimuth limitations may be waived. The velocity requirement stated in Figure 2-1 assumes that such a waived launch azimuth limitation is obtained for a Scout E launch from Wallops Island directly into a  $63.4^\circ$  orbital inclination with an initial 185 km parking orbit.

For a  $63.5^\circ$  inclination launch from Wallops Island the associated velocity penalty (due to rotation of earth)  $\Delta V_3 = .2$  km/sec. The total characteristic velocity requirement therefore  $V_T = V_1 + \Delta V_1 + \Delta V_2 + \Delta V_3$  where  $V_T = 7.8$  km/sec. + .3 km/sec + .15 km/sec + .2 km/sec;  $V_T = 8.447$  km/sec. The corresponding payload capability for this characteristic velocity delivered by a Scout E is about 150 kg.

The assumption of an azimuth launch within range safety limitations and directly into desired altitude eccentricity (requiring an orbital plane change) results in a considerably lower payload capability,  $\approx 120$  kg maximum.

#### A.4 Orbital Lifetime Evaluation

Earth oblateness and atmospheric drag are the two primary factors contributing to the orbital lifetime of near earth satellites although anticipated orbital altitudes of this experiment appear to be above that which is considered "near earth", it is felt necessary to perform a projected time at which the elliptic orbit is reduced from 1333 km x 660 km to 1000 km x 666 km.



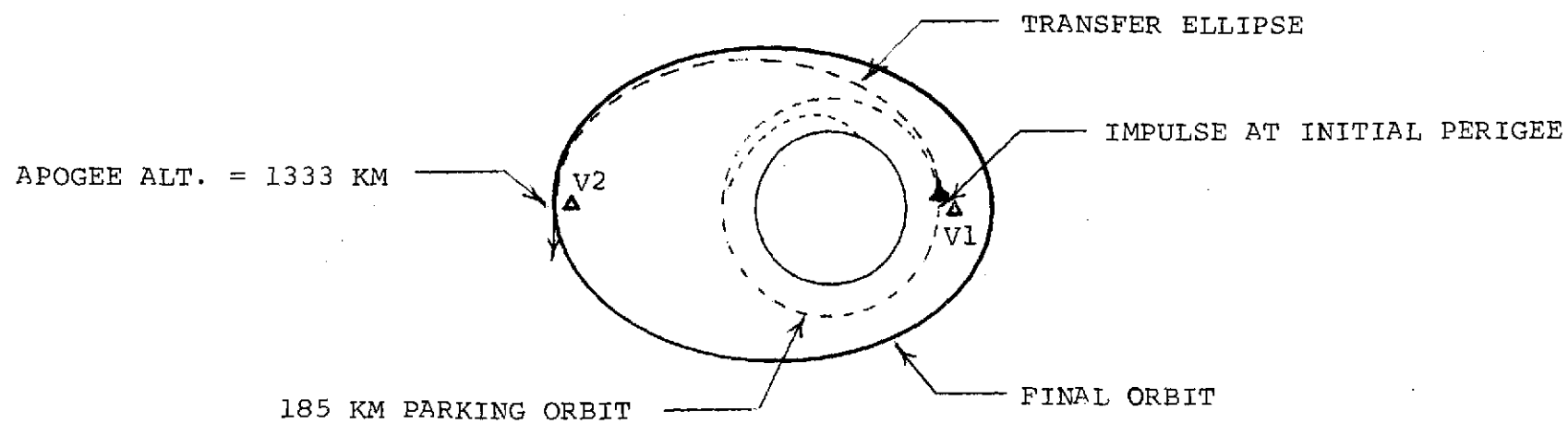


FIGURE A-1 ORBITAL MANEUVERS

#### A.5 Spacecraft Lifetime Considerations

Two basic means of obtaining a first approximation of the useful lifetime of a spacecraft are available to the spacecraft design engineer:

- 1) Analytical closed form solution and
- 2) Numerical integration of orbital decay rates

Post experience has shown that the closed form analytical solutions have one or both of the following inherent limitations:

- 1) An insufficient number of terms is carried in the series expansions.
- 2) The total lifetime is based completely on the initial atmospheric conditions (i.e. density at initial perigee altitudes, initial logarithmic density lapse rate, etc.)

Based upon the fact that numerical integration of orbital decay rate has shown greater accuracy, this approach is used here to obtain an estimated orbital lifetime.

Using a combination of Perkin method and Bessel expansion, orbital decay rates may be determined through a numerical analysis. These apogee-perigee decay rates are fed into a computer in tabular form. For small altitude increments the

following expression although applicable to circular orbits is similar to that for orbits of small eccentricity.

$$\Delta t_j = \frac{\Delta h_j}{\left(\frac{dh}{dt}\right)_j}$$

where

$$\Delta h_j = j^{\text{th}} \text{ altitude decrement}$$

$$\left(\frac{dh}{dt}\right)_j = \text{decay rates at their altitude}$$

Total lifetime is found by the summation of all time increments up to impact

$$L_t = \sum_{j=0}^{\text{impact}} \Delta t_j$$

The resulting lifetime curves are plotted on logarithmic scale versus initial eccentricity in Figure I-1 based on an ARDC 1959 atmospheric density model and a ballistic coefficient

$$B = \frac{C_D A}{2m} = 1.0 \text{ FT}^2/\text{SLUG}$$

where:  $C_D$  = drag coefficient of the satellite  
 $\approx 2.75$

$A$  = projected surface area ( $\text{FT}^2$ ) = 13  $\text{FT}^2$

$M$  = satellite mass (SLUGS) = 10.27

In this case:

$$h_p \cong 400 \text{ statute miles}$$

$$e = 0.045$$

$$B = 1.75$$

Referring to the figure based on this information yields an approximate lifetime

$$L_t = 40,000 \text{ days normalized to } B=1.0\text{FT}^2/\text{SLUG}$$

Therefore the total lifetime estimate is given by

$$L_t = \frac{40,000}{1.75} = 22,854 \text{ days}$$

$$\text{or } L_t \cong 62 \text{ years}$$

While orbital lifetime predictions have in the past proved to be relatively inaccurate it can be believed with confidence that because this orbit is not "near earth" the lifetime expectancy can be considered to be at least an order of magnitude above the required lifetime of the experiment.

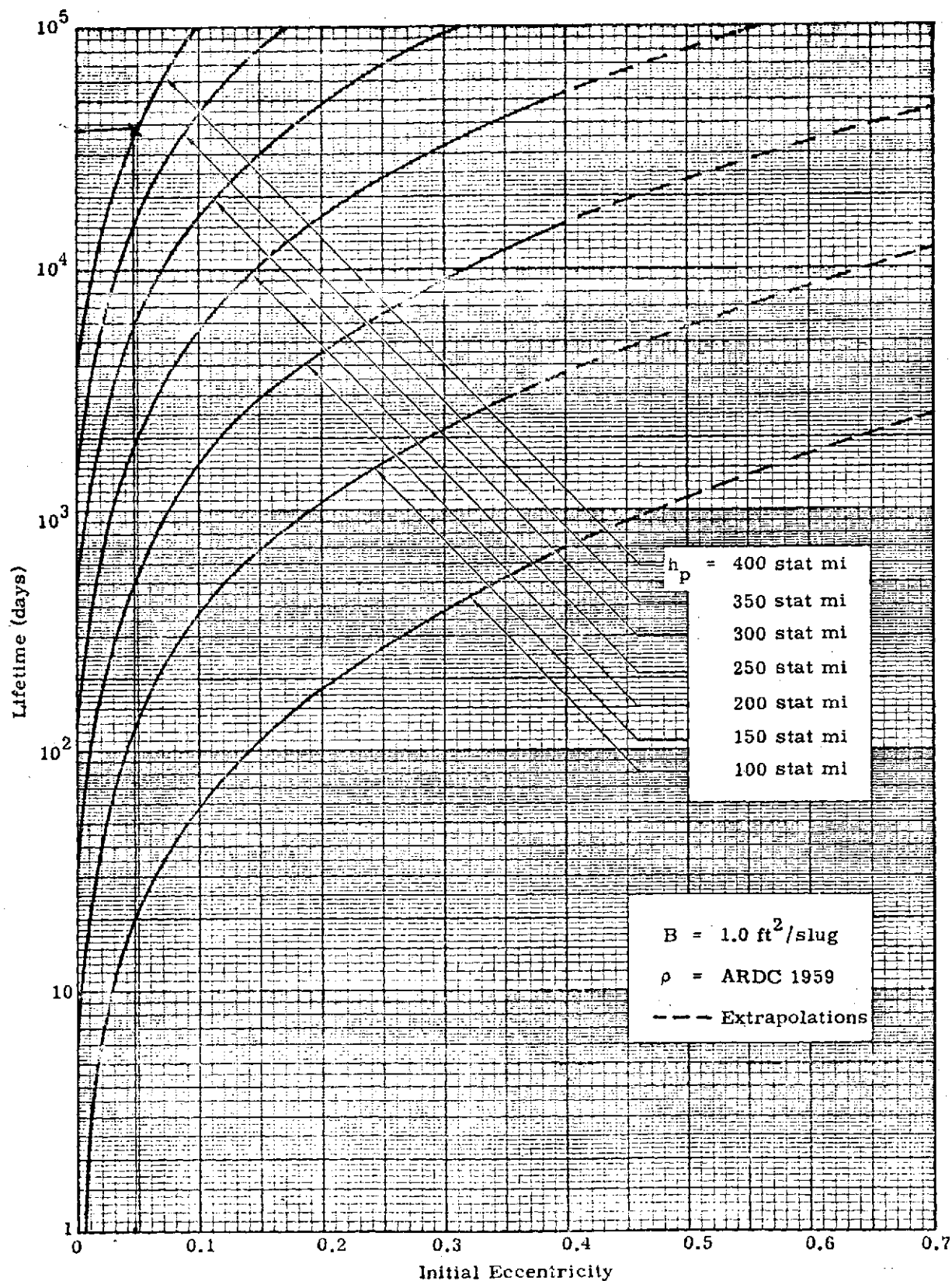


FIGURE I-1 SATELLITE LIFETIME VERSUS INITIAL ECCENTRICITY

APPENDIX B

EXPERIMENT MANAGEMENT

## B. EXPERIMENT MANAGEMENT

The man-made noise experiment will constitute a project of significant time, money and output. It will serve and interface a number of "customers" throughout the Federal establishment, other levels of government, and in the private sector (e.g., COMSAT). It is reasonable to assume, therefore, that the project will be managed, from some point during its definitive stages, by a dedicated organization structured to the specific needs of the project. To provide an initial baseline for consideration, such an organization is postulated here.

The initial study leading to project definition and budgeting will likely be completed by existing organizations; the project committed organization will not come into being prior to the initial funding of the satellite experiment. (It is likely that aircraft flown "versions" of this experiment will have been undertaken prior to the orbiting "version" if only to demonstrate its feasibility).

Major tasks required in connection with the experiment, which will require dedicated management, will include:

Experiment hardware specification, design and fabrication:

Receiver;

Low frequency broad-beam antenna;

High frequency broad-beam antenna;

High gain antenna;

Magnetic tape recorder;

Antenna controller;

Launch vehicle selection and preparation; System integration:

- Spatial;
- Mecahnical;
- Thermal;
- Electrical;
- Electromagnetic;
- Signal;
- Test;

Scheduling:

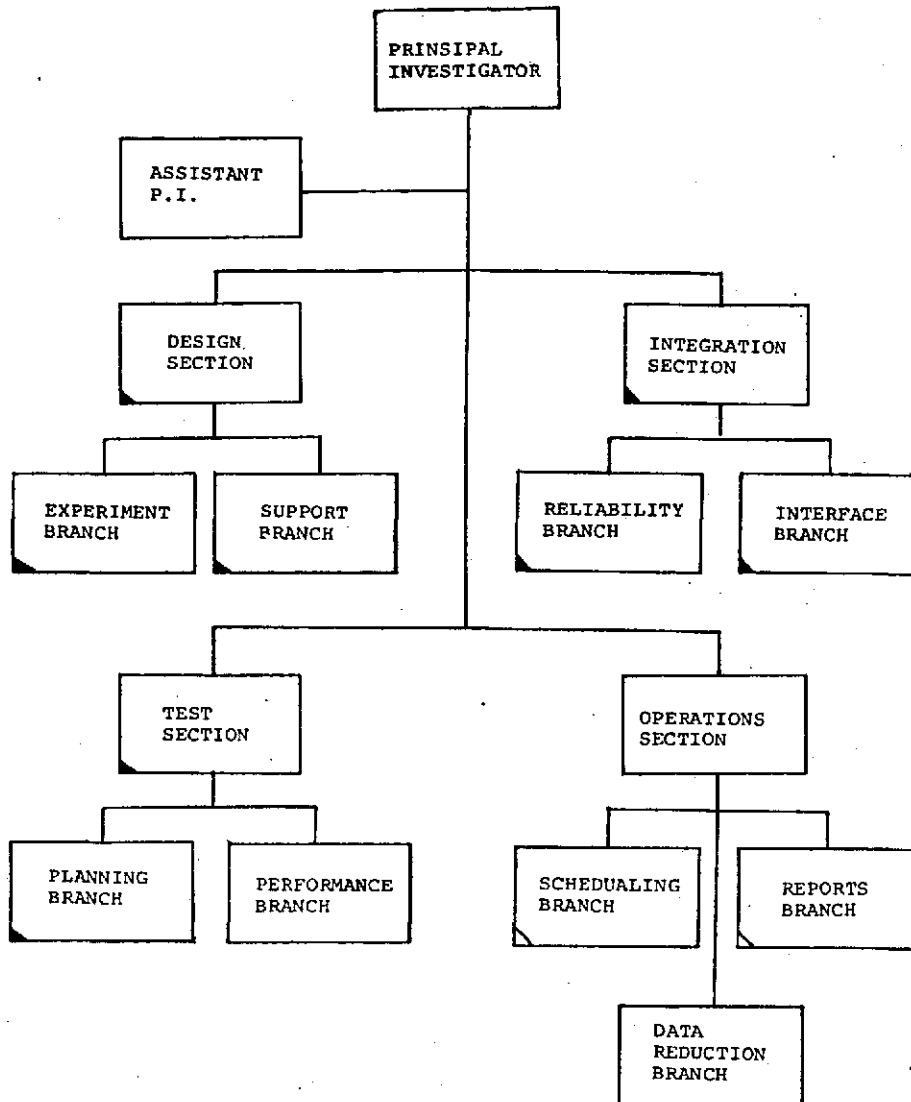
- Design and integration;
- Launch;
- Test;
- Ground station support;
- Data processing;

Data reduction and analysis:

Report preparation.

The personnel requirements for these tasks will cover a wide range. The performance periods will vary extensively; some will consist entirely of pre-launch activities, and others will perform after the launch only. A logical and efficient organizational structure for management of these tasks and functions might be as indicated in Figure B-1. The structure of this organization would alter with the course of the project, but the principal investigator and other key personnel would maintain





	REP-LAUNCH	POST-LAUNCH
PERSONNEL	40	24
ANNUAL SALARIES	\$500k	\$410

- ☐ indicates functional throughout project
- ☐ indicates functional prior to launch only
- ☐ indicates functional after launch only

FIGURE B-1 MAN-MADE NOISE EXPERIMENT PROJECT OFFICE

their respective positions throughout the course of the project. Figure B-1 also presents estimates of personnel and direct annual salary requirements for the postulated organization.

Figure B-2 offers a schedule outline for the experiment, indicating major categories of effort and periods required for them.

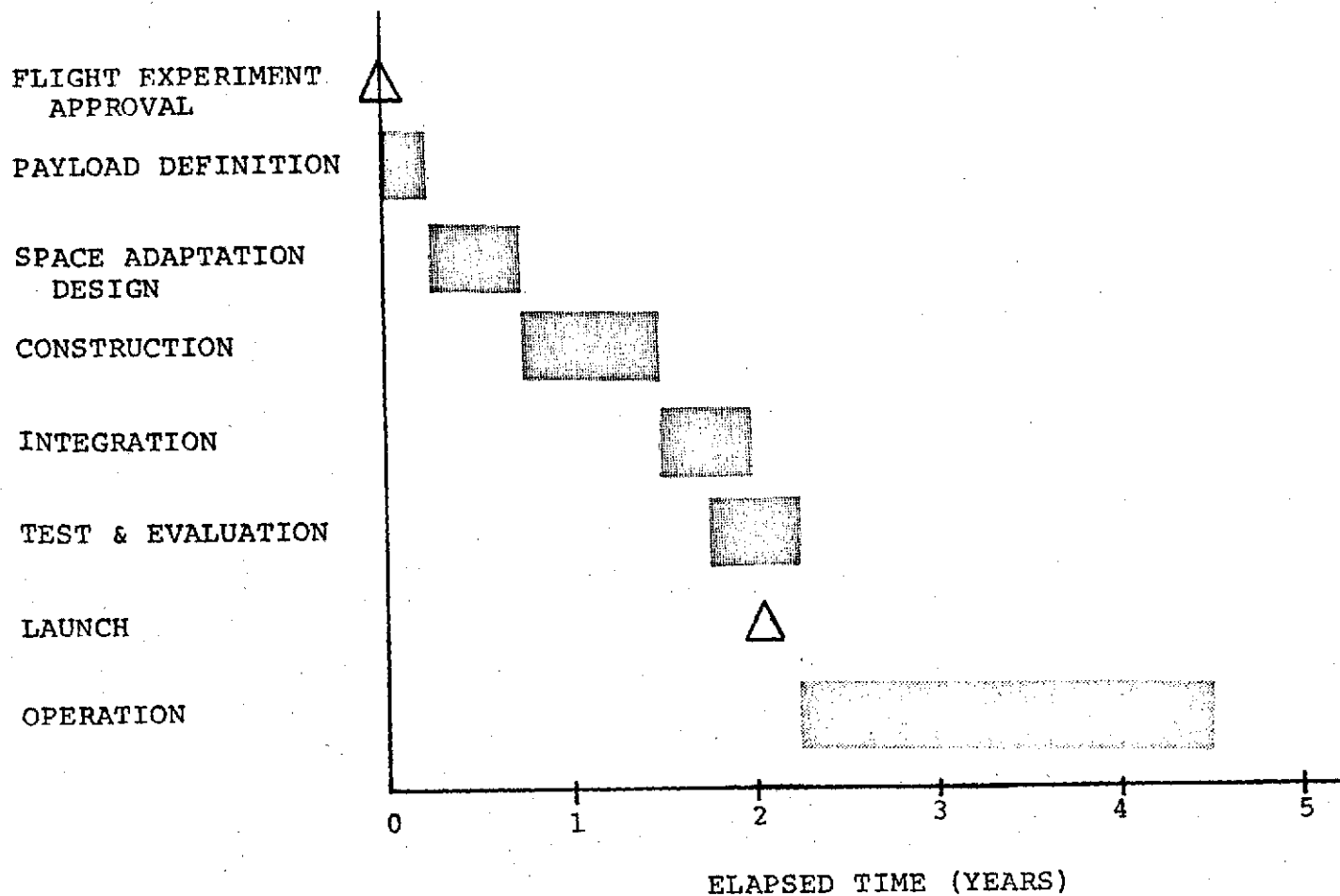


FIGURE B-2 MAN MADE NOISE EXPERIMENT PROJECT SCHEDULE

APPENDIX C  
RECEIVER SCANNING CONSIDERATIONS

1. The AAFE Man Made Noise Experiment receiver, operating in one of its standard modes will repetitively scan a band of frequencies determined by ground command. A number of considerations relating to its scanning or sweeping function are discussed below.
2. The proposal upon which this project is based<sup>1</sup>, assumes the use of incremental tuning for the receiver, but in discussions with the NSL staff, Mr. John Thomson, the COTR, has suggested continuous swept tuning as a desirable method of scanning. He also questioned the ability of the receiver to complete multiple scans in a single "pass".
3. There is no literature at hand which specifically addresses the choice of incremental vs. continuous tuning for receivers of the type to be designed. The experiment design proposed for the ATS-F and G spacecraft<sup>2</sup>, proposes a wideband transponder in the spacecraft and spectrum analyzers at the ground stations; demodulation is accomplished on the ground using swept spectrum techniques, and no quantizing and digital processing was anticipated. Similar hardware and techniques were applied during the General Dynamics NASA ground and airborne measurement and analysis program.<sup>3,4</sup> The General Dynamics 200-mile orbit feasibility study<sup>5</sup> is also based on swept frequency tuning, although "interrupted tuning" approaches are mentioned briefly. However, since this study is based on the use of a manned spacecraft and onboard, human operation, data processing and analysis, its relevance to the present case is minimal. The GSFC RFI receiver specification<sup>6</sup> requires incremental tuning, but the rationale for the requirement is not

presented in the specification. The AIL receiver proposal<sup>7</sup>, based on the GSFC specification cited above, discusses only the incremental tuning approach using a frequency synthesizer. Other studies and experiments involving automatically tuned receivers have been reviewed, but none discuss the trade-offs between continuously swept and incremental tuning methods.

4. One report<sup>8</sup> includes a germane discussion of acquisition probability; it is the final report of a study concerning a wide variety of interference measurement and surveillance techniques through the 100 kHz to 40 GHz range. The main point of this discussion is that the greatest probability of acquisition by a sweeping receiver of a pulsed, coherent emission source with a rotating antenna requires minimizing receiver dead-or blanking-time per sweep. (The use of an equal rise- and fall-time sweeping waveform is suggested, but is then discounted because of the hysteresis effects in voltage tuned components such as YIG filters.) The experiment under design at the present time will, in all likelihood, include bands wherein the aggregate power will include high level pulses from antennas peripherally visible to the spacecraft for very brief periods (owing both to spacecraft track and emitter antenna rotation, e.g., radar bands). Because their contributions may be highly significant from an interference standpoint, care must be taken to assure that the probability of acquisition by the spacecraft receiver is high. For each receiver frequency increment, there may be an associated blanking period to facilitate oscillator settling; if this be the case, continuous sweeping will eliminate the need for such blanking and thereby enhance the probability of

acquisition for all significant emissions encountered. Hence, the only text available which relates to trade-offs between incremental and continuous tuning tends to point toward continuous tuning as a better choice, if incremental tuning requires blanking for each increment. There may, however, be other factors in the choices which remain to be considered; it may be that there have been substantial and relevant reasons for the choice of incremental tuning in a number of previous spectral analysis experiments. Further consideration of the question is in order, particularly as regards sampling and digitizing effects, data precision and the like.

5. The ability of the receiver to complete multiple scans detecting a given emitter in a single pass (to provide doppler information) will depend upon the proximity of the emitter to the track of the spacecraft, the size and shape of the spacecraft antenna footprint, antenna sidelobes, spacecraft altitude, orbit eccentricity, spacecraft receiver scan rate, scanning spectrum, etc. More simply stated, the number of times an emitter is afforded the opportunity to be detected during a pass is dependent on the period it is in view by the spacecraft and the rate at which its frequency is scanned. The period in view is dependent on the track and dynamics of the spacecraft orbit and may fall anywhere from a maximum value to zero. The rate at which any frequency is scanned is determined by the fundamental scanning rate (Hertz per second) and the width of the scanned band (Hertz).

6. The period of illumination by a terrestrial emitter of an orbiting spacecraft during a single pass, or orbit, may range from zero to the entire orbit period. (The former value results from an orbit pass during which the emitter does not come into the spacecraft field of view; the latter from an emitter in view of a spacecraft in geostationary orbit). Major determinants of illumination period include spacecraft orbit altitude, orbit inclination, and minimum distance from emitter to track.\* The maximum illumination period of an object (for sun-synchronous orbit spacecraft) occurs when the terrestrial emitter lies on the orbit track directly beneath the apogee, and the spacecraft is in a direct (prograde) zero inclination orbit (hence, the emitter lies on the equator, and the orbit is equatorial). By way of example, the absolute maximum illumination period of 1000 km altitude satellites is approximately 19.0 minutes. The maximum viewing period decreases with inclination angle; for the case of a polar 1000 km orbit, maximum illumination period is approximately 17.5 minutes; for a  $180^\circ$  inclination 1000 km orbit, 16.4 minutes. A considerable contribution to the aggregate flux density at the satellite position will likely occur at times from emitters near the limb, at its furthest distance from the track of the satellite. This likelihood results from the generally horizontal radiation patterns of many terrestrial

---

\*For elliptical orbits, a number of orbit parameters may also have considerable effects on illumination periods. However, for orbits with low order eccentricities ( $<.05$ ), mean-altitude circular orbit calculations provide adequate approximation values. The eccentricity of a 1000 km mean altitude elliptical orbit with an apogee to perigee altitude ratio of 2:1 is .045.



emitters (e.g., broadcast TV; search radar; LOS relay); their maximum gain intersections with the orbital sphere occur from the satellite horizon. The periods of illumination by such emitters will be very brief, but their numbers and their overall significance as interferors is expected to be appreciable. Acquisition by the experiment of these interference signals is very desirable, lest resulting data be appreciably different from that produced by continuous coverage at each frequency. Hence, if only the on- and near-track emitters were consequential, illumination periods of 15-18 minutes would provide a basis for setting scan rates and frequency dispersions; consideration of all "high-level" contributors to the interference environment at each position and frequency on the orbital sphere, however, tends to reduce the "basic period" to a smaller value.

7. The maximum rate at which a scanning receiver may operate without unacceptable loss of definition (i.e., apparent carrier sensitivity and apparent resolution) is determined by the relationships:<sup>9</sup>

$$\alpha = \frac{1}{[1 + (\frac{2 \ln 2}{\pi})^2 (\frac{f_s}{t_s \Delta f})^2]^{1/4}}$$

and

$$\frac{\Delta f_{\text{eff}}}{\Delta f} = [1 + (\frac{2 \ln 2}{\pi})^2 (\frac{f_s}{t_s \Delta f})^2]^{1/2}$$

where:  $\alpha$  = loss in carrier response, maximum response/response  
 $f_s$  = frequency scanning range (dispersion range)  
 $t_s$  = scanning period  
 $\Delta f$  = receiver bandwidth, and  
 $\Delta f_{\text{eff}}$  = apparent bandwidth

These relationships are plotted in Figures 1 and 2. It is apparent that, where  $f_s/t_s \leq \Delta f^2$ , neither response nor resolution are appreciably affected. Other pertinent relationships are indicated in Figures 3 and 4. Figure 3 indicates scan rate as a function of normalized scan rate,  $[f_s/(t_s \Delta f^2)]$ , for selected receiver bandwidths. Figure 4 relates scan period and bandwidth where  $f_s/t_s = \Delta f^2$  for various bands. It is worthy of note that a 12 GHz band, the entire spectrum of interest, could be scanned without appreciable loss of sensitivity or carrier resolution, in a period of one minute with a receiver bandwidth less than 20 kHz. Unfortunately, other more stringent limitations bear on scanning rate for the present experiment; the considerations just discussed are pertinent for "high fidelity" analogue outputs only (e.g., spectrum analyzer displays). The down-link data stream from the Man-Made Noise Experiment receiver will be power limited, and appreciable bandwidth or noise penalties resulting from this limitation must be considered.

8. It is not an objective of this experiment to investigate the modulation envelopes or spectral characteristics of individual terrestrial interference sources; hence the need and desirability of broadband analogue down-link channels are obviated. However,

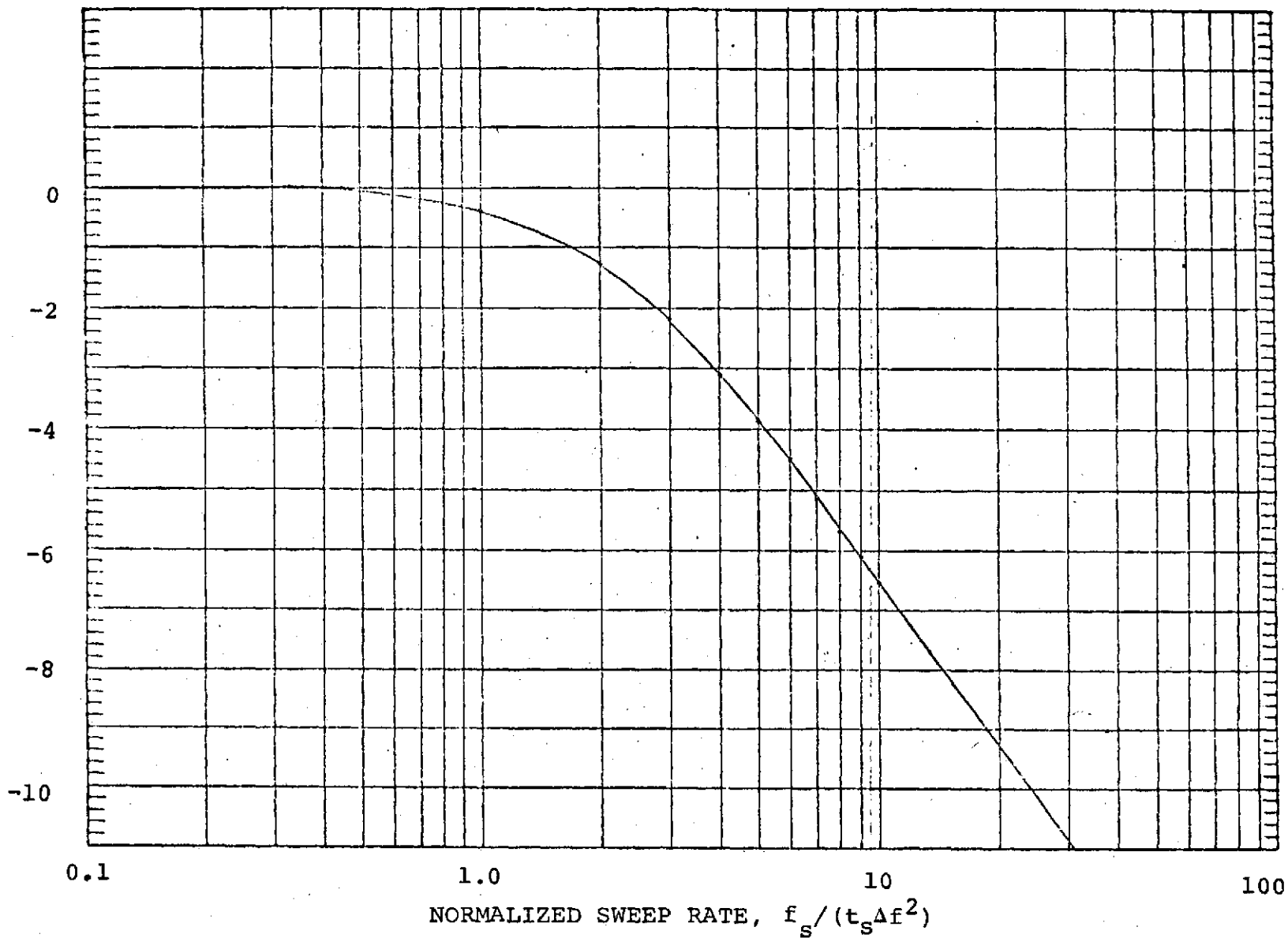


FIGURE C-1 SCANNING RECEIVER CARRIER RESPONSE VS SCAN RATE

EFFECTIVE BANDWIDTH RATIO,  $\Delta f_{eff}/\Delta f$

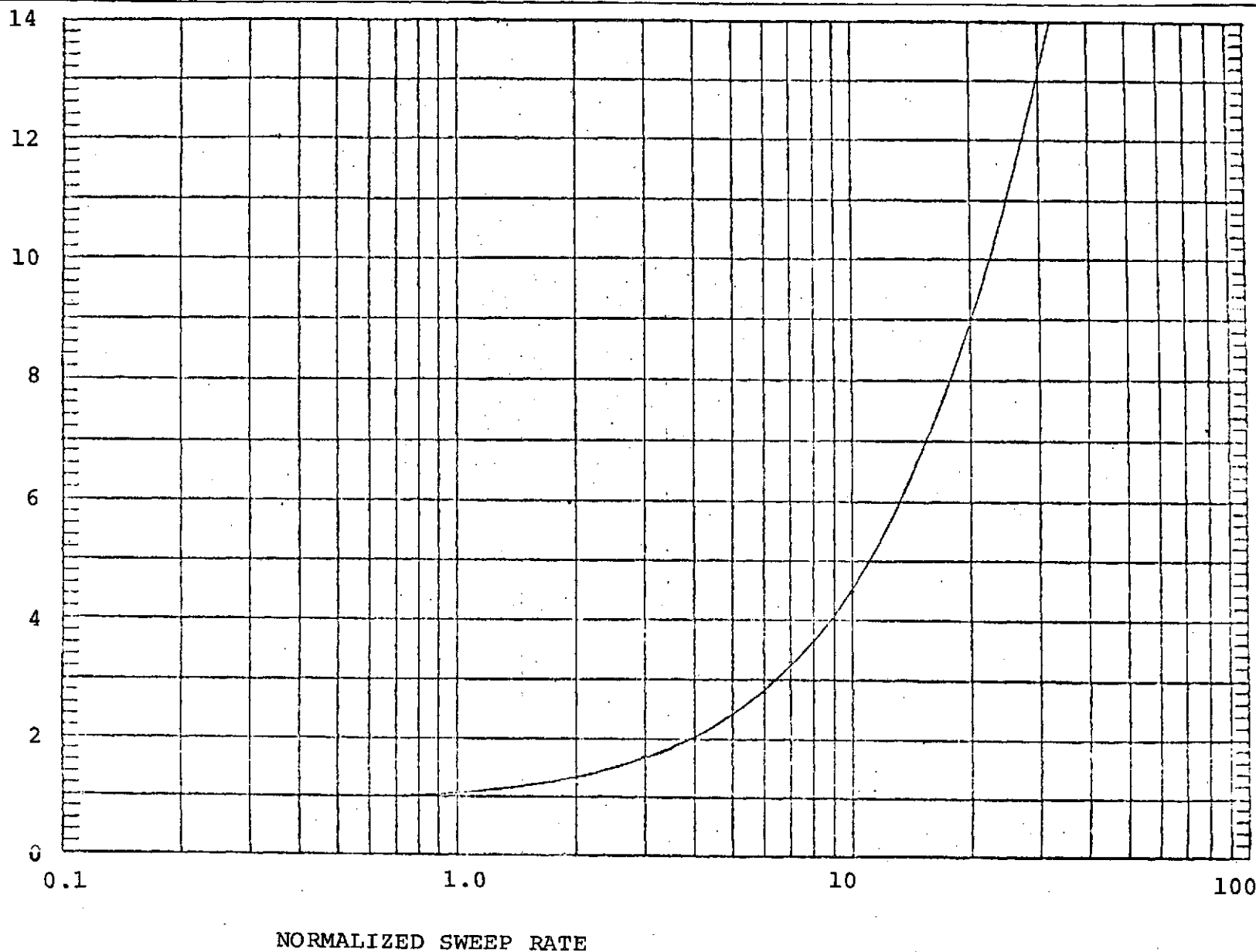


FIGURE C-2 SCANNING RECEIVER RESOLUTION VS SCAN RATE

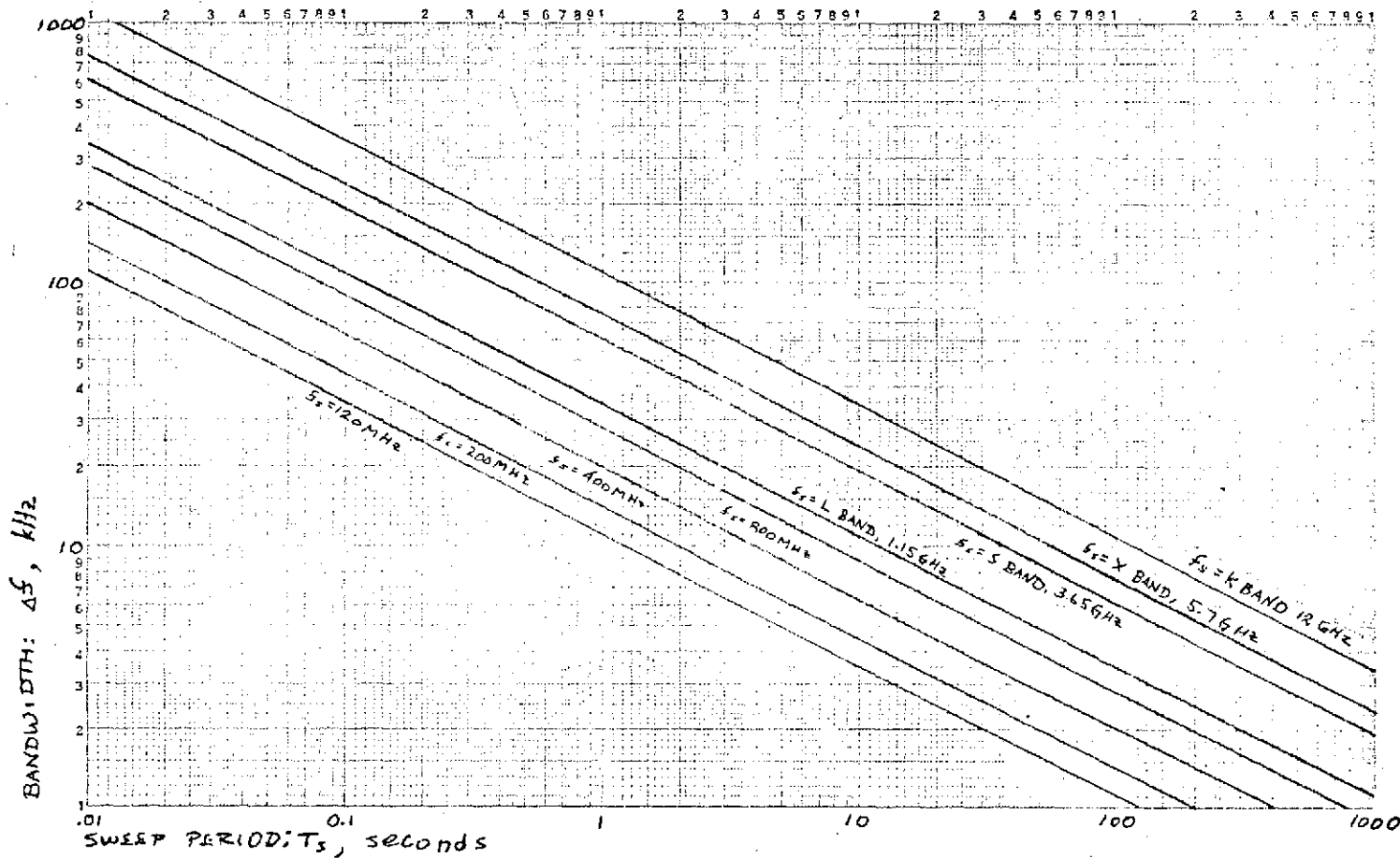


FIGURE C-3 SCANNING RECEIVER SCAN PERIOD VS BANDWIDTH,  $F_s/T_s = \Delta F^2$

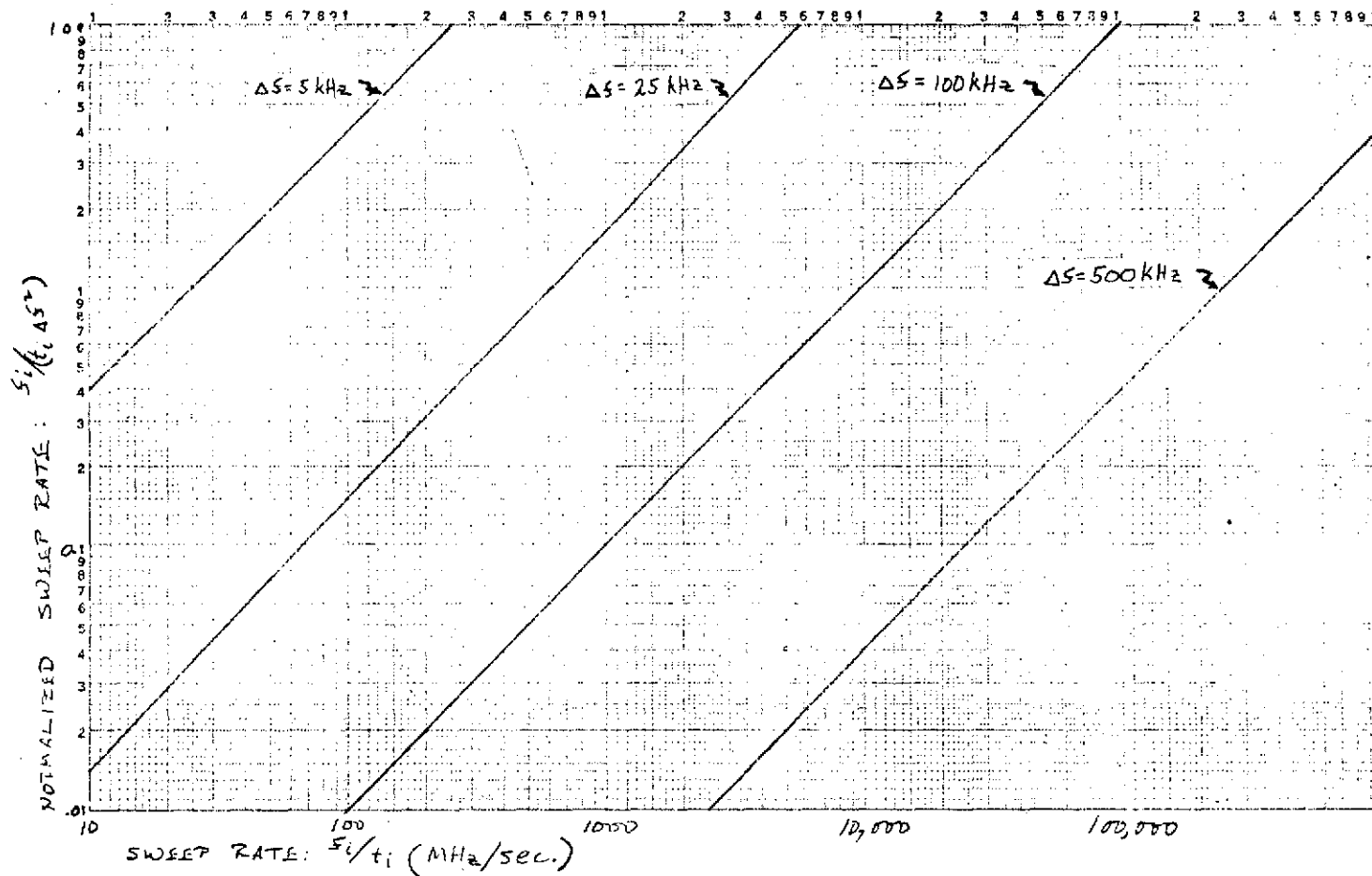


FIGURE C-4 SCANNING RECEIVER SCAN RATE VS "NORMALIZED" SCAN RATE

the desirability of "easy" interface with existing and planned NASA data link facilities and of power constrained channels is readily apparent, and suggests the use of digital experiment data down-link transmission format, as does the obvious requirement for extensive post-pass experiment data processing. It appears feasible to assume a maximum down-link experiment data rate of 51.2 kb/sec., that of the Unified "S-Band" (USB) high-speed telemetry data channel; USB links are compatible with all major STADAN stations and will remain so for the foreseeable future. Based on the 51.2 kb/sec. constraint, the maximum number of amplitude data samples, per second  $S/\text{sec} \approx (51.2 \times 10^3)/B_s$ , where  $B_s$  = bits/sample (b/s). The bit requirements per sample is determined by amplitude resolution requirements and the amplitude dynamic range of the data, both of which can be expressed in dB. Assuming a dynamic range  $\geq 70$  dB per sample and amplitude resolution requirements of 1 dB, the number of bits required is 7 per sample. Hence, the maximum number of data samples per second,

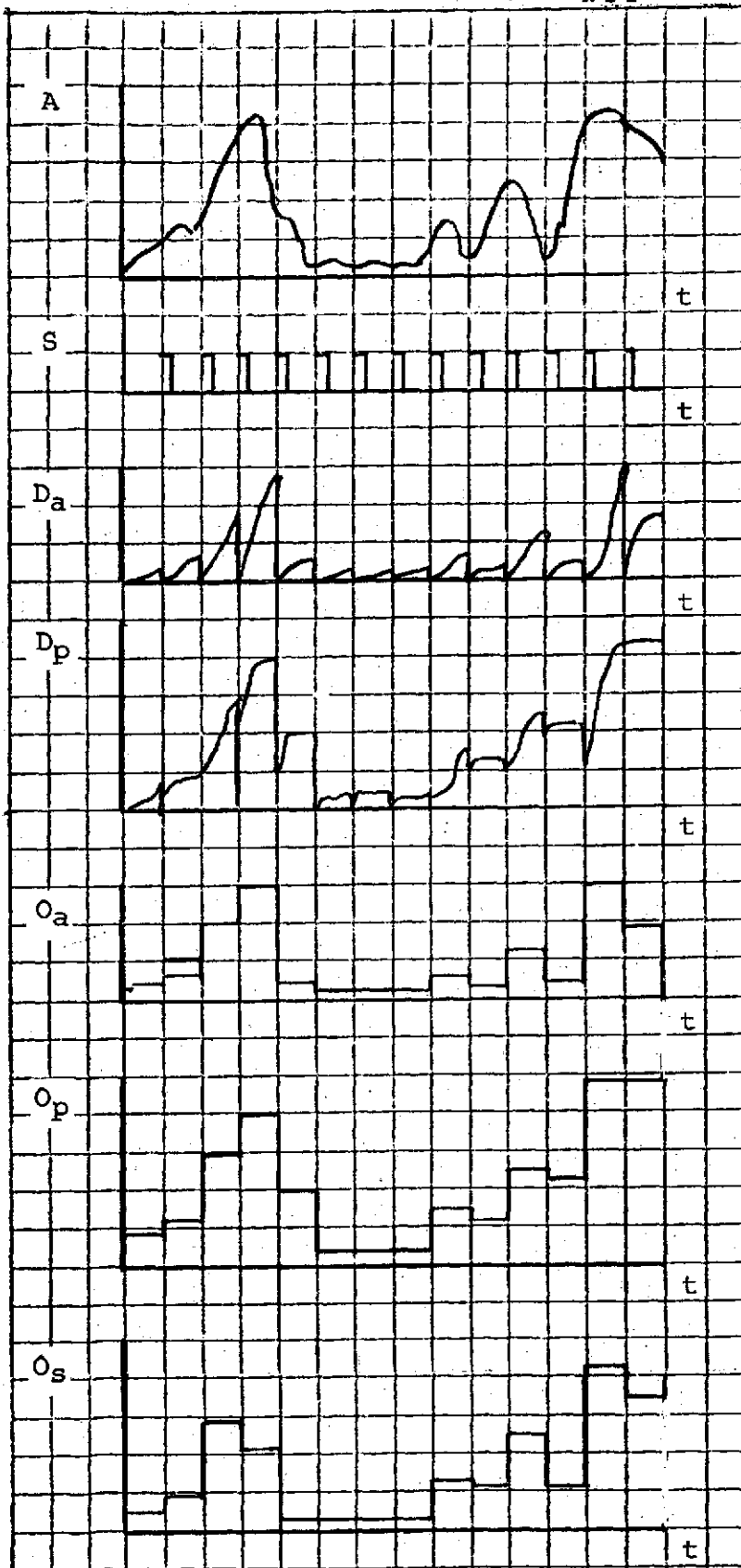
$$(S/\text{sec})_{\text{max}} \approx (51.2 \times 10^3)/7 = 7.2 \times 10^3$$

9. With a fixed maximum data sampling rate the sampling characteristic, the receiver resolution (carrier bandwidth) and the receiver scan rate determine the relationship between analogue receiver IF output and down-link data. This relationship is of great import to the data analysis. For example, among the possible data sampling characteristics are:

- o Peak amplitude value during sample period;
- o Average amplitude value during sample period;
- o Instantaneous value at sample time;
- o Average value rate of change during sample period.

(Of course, other sampling functions might also be considered, including those combinational forms wherein the output data would represent two values resulting from the same sample). Figure 5 is a sketch representing the time functions of a hypothetical receiver output with various sampling functions applied. Figure 6 is a like representation for a case with a receiver  $\Delta f/t_s$  considerably lower than that of Figure 5. These sketches indicate likely differences between data records for three possible sampling functions. Figure 7 relates the graphic presentations of Figures 5 and 6 to a functional block diagram in which, each of the three functions operate via its own channel. It is noteworthy that if the lower  $\Delta f$  ( $t_s \leq 0.5$ ) were represented in compliance with the Nyquist sampling criterion, the records would present identical forms. In that case, the form of the representative data records would essentially be that of the IF output signal itself, and could be used to yield an analogue reconstruction of the original output signal. However, with a 7 bit/sample down-link data word, the sampling criterion requires  $\Delta f \leq B_T/14$  where  $B_T$  is the down-link data rate in bits per second (b/sec). With a 51.2 kb/sec. channel, receiver bandwidth would be limited to 3.66 kHz ( $\Delta f \leq 0.5$  s/t), and the maximum rate of scan would be 13.4 MHz/sec. ( $f_s/t_s \leq \Delta f^2$ ). To return to the central issue of the paragraph, however, the relationship between the earth station data record and the receiver





IF AMPLITUDE AT DETECTORS

SAMPLE AND RESET PULSES  
APPLIED TO DETECTORS AND  
TO A/D CONVERTERS

AVERAGING DETECTOR OUTPUT

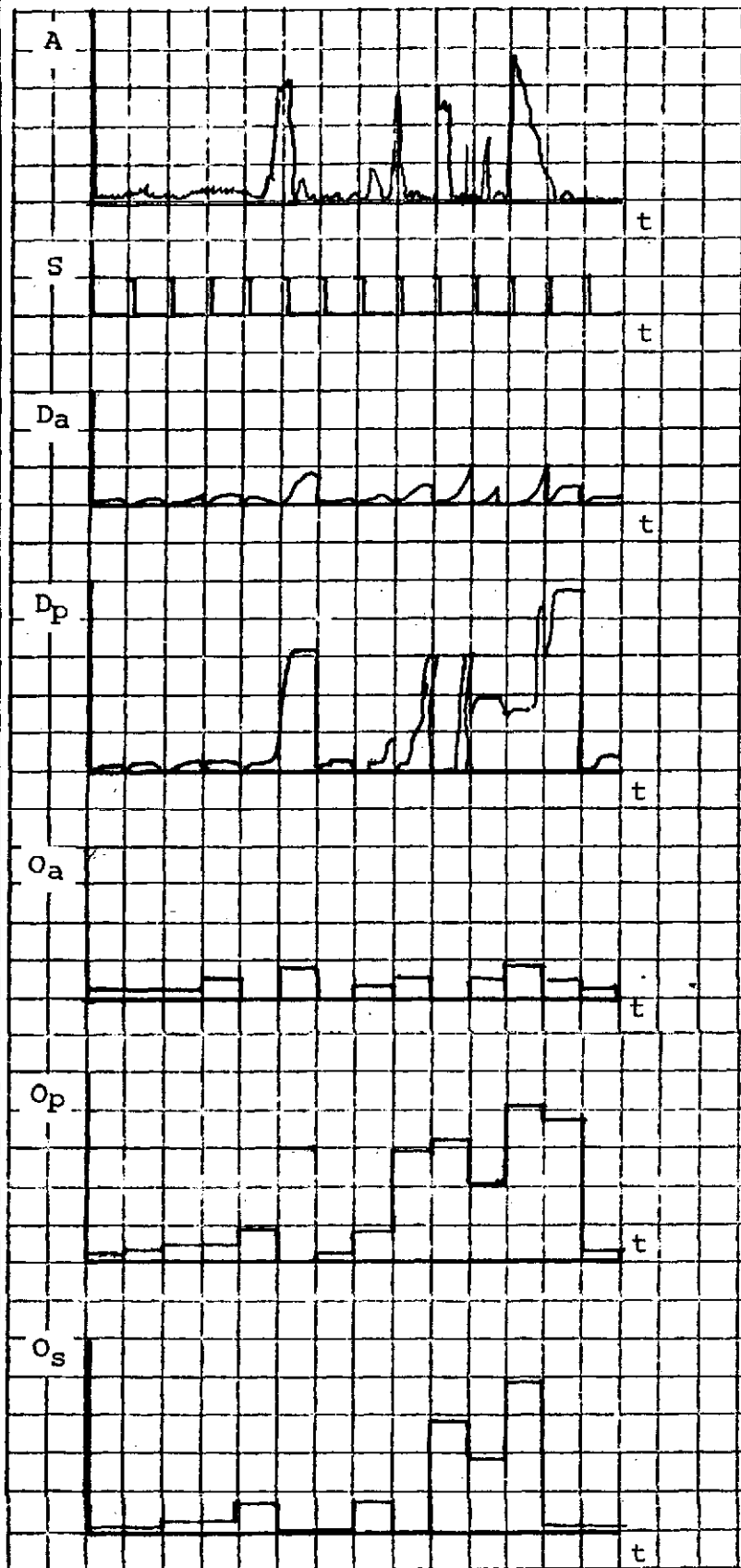
PEAK DETECTOR OUTPUT

AVERAGE DATA OUTPUT AT  
EARTH STATION

PEAK DATA OUTPUT AT  
EARTH STATION

INSTANTANEOUS SAMPLED  
DATA AT EARTH STATION

FIGURE C-5 PLAUSIBLE EXAMPLES OF ORIGINAL DATA AND  
CONTROL SIGNALS:  $\Delta f \approx 2S/t$



IF AMPLITUDE AT DETECTORS

SAMPLE AND RESET PULSES  
APPLIED TO DETECTORS AND  
TO A/D CONVERTERS

AVERAGING DETECTOR OUTPUT

PEAK DETECTOR OUTPUT

AVERAGE DATA OUTPUT AT  
EARTH STATION

PEAK DATA OUTPUT AT  
EARTH STATION

INSTANTANEOUS SAMPLED  
DATA AT EARTH STATION

FIGURE C-6 PLAUSIBLE EXAMPLES OF ORIGINAL DATA AND  
CONTROL SIGNALS:  $\Delta f \gg S/t$

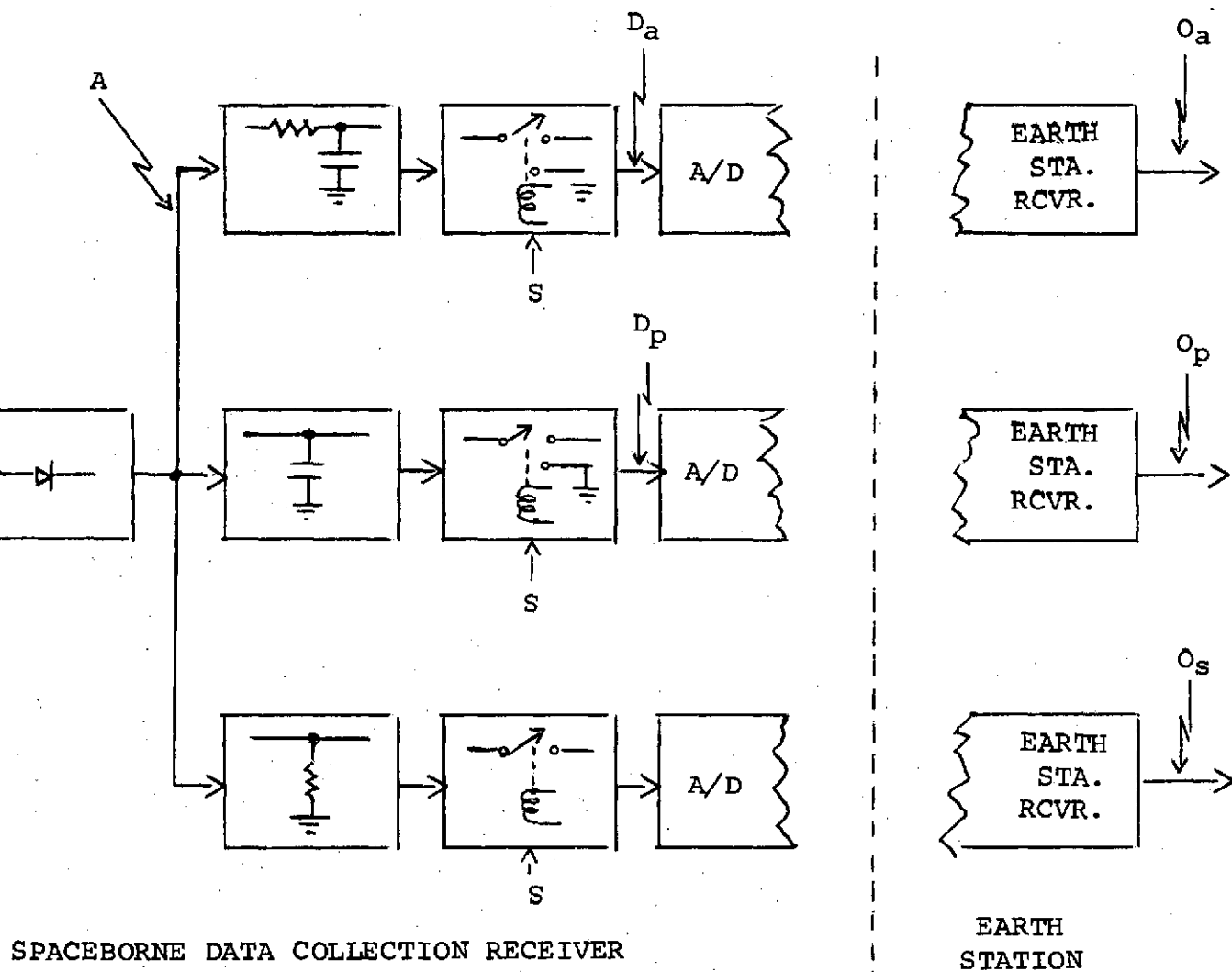


FIGURE C-7 HYPOTHETICAL DATA COLLECTION SYSTEM, PARTIAL BLOCK DIAGRAM

output are determined by the sampling characteristics, resolution, and scanning rate. The optimum properties for these parameters will be determined by relating goals for dispersion, sensitivity and permissible frequency error.

10. For the present experiment, dispersion may take any value between 0 and 11.6 GHz. However, the problems and penalties resulting from rapid antennae switching and other considerations relating to both hardware and data processing, are likely to preclude full range dispersion as a normal mode of operation. Dispersion selections occupying as much as the entire range of a single experiment antenna, however, may well be desirable; if the log-periodic antenna structure is employed, a maximum range on the order of 4 GHz may be plausible. Hence, 4 GHz is considered as the maximum dispersion in the normal scanning mode of operation.

11. The sensitivity of the receiver must be adequate to permit accurate measurement of potential interferors by the spaceborne system. The operating temperature, or noise figure, of the receiver will be constrained by current RF amplifier state-of-the-art, but cw sensitivity can be optimized by static receiver bandwidth (i.e., the receiver passband characteristic measured when it is not scanning) and limitation of maximum scan rate to the  $f_s/t_s \leq \Delta f^2$  value. It appears that the best achievable front-end performance for the receiver will be  $NF \approx 10$  dB. Based on  $\bar{N}_i = kTB$ , where  $T = \sim 90$  [antilog (NF/ID)]-290, the cw sensitivity of the receiver can approximate:

$\bar{N}_i$	$\Delta f$	$(f_s/t_s)_{\max}$
-133 dBW	1 MHz	1000 GHz/sec
-143 dBW	100 kHz	10 GHz/sec
-149 dBW	25 kHz	625 MHz/sec
-153 dBW	10 kHz	100 MHz/sec

If the receiver input transducer is a paraboloid/sec antenna of  $A_e \approx 1 \text{ m}^2$  ( $D \approx 1.5 \text{ m}$ ), for a minimum  $S_i/\bar{N}_i = 3 \text{ dB}$ , the power flux density of a carrier at the satellite must be  $\text{PFD} \geq -130 \text{ dBW/m}^2$  with  $\Delta f = 1 \text{ MHz}$ , or  $\text{PFD} \geq -150 \text{ dBW/m}^2$  for  $\Delta f = 10 \text{ kHz}$ . The use of a non-directional antenna of constant gain would make the antenna effective area frequency dependent,  $A_e \text{ (dB ref } 1 \text{ m}^2) = 38.5 + G(\text{dB}) - 20 \log f_o(\text{MHz})$ . Typical gain for a wide beam "frequency-independent" antenna is 6 dBi. The effective area of such an antenna is  $A_e = -7.5 \text{ dB ref } 1 \text{ m}^2$  at 400 MHz;  $A_e = -37 \text{ dB ref } 1 \text{ m}^2$  at 12 GHz. At a distance of 4000 km, the nominal slant range to the horizon for a satellite at 1000 km altitude, propagation spreading loss is  $L_s \approx 143 \text{ dB}$ . Hence, for a receiver with a 1 MHz bandwidth at 1000 km altitude, the minimum detectable e.i.r.p. from the horizon with a 6 dB antenna will be on the order of 50 dBW at 12 GHz; 21 dBW at 400 MHz.  $(\text{e.i.r.p.}_{\min} \text{ (dBW)} = \text{PFD}_{\min} \text{ (dBW/m}^2) - A_e \text{ (dB ref } 1 \text{ m}^2) + L_s$ ). If the receiver bandwidth is reduced to 25 kHz, the minimum detectable cw e.i.r.p.'s will be decreased by 16 dB; or 34 dBW at 12 GHz; -13 dBW at 400 MHz.

12. Another consideration which will bear on minimum bandwidth for the receiver is the aggregate spectra and stabilities of signals to be measured; it will decrease sensitivity to limit the passband of the receiver so much as to reject appreciable signal energy. The modulation of potential interferers will vary over wide ranges or values. Radar, tropospheric scatter links, wide-band LOS communications links, and television spectra will be measured in MHz; voice and low speed data links in the mobile and aeronautical services occupy much "narrower" channels. The levels of conventional radar, troposcatter and broadcast television will be adequate for detection with a relatively narrow-band receiver because of their very high e.i.r.p.'s. LOS communication links, however, may be marginal or undetectable with low gain antennas. The typical LOS e.i.r.p. is 40 dBW, and its spectrum is 20 MHz. The distribution of energy is not uniform through that band, however, and frequently is heavily concentrated about the carrier. The source stabilities of interference signals will be on the order of 1 part in  $10^6$  or better (except for some mobile cases), but doppler effects can be considerable. The doppler problem is worthy of further consideration, but for first approximation purposes, a 1000 km orbit may produce overhead pass doppler shifts on the order of  $\pm 280$  kHz at 12 GHz, and  $\pm 10$  kHz at 400 MHz.

REFERENCES

1. Technical Proposal: Man-Made Noise Experiment, NSL, PN 704A, January 1972.
2. Henry, V. F. and Kelleher, J. H.: Radio Frequency Interference Experiment Design for the Applications Technology Satellite, NASA TN D-5041, May 1969.
3. Mills, A. H.: Measurement and Analysis of Radio Frequency Noise in Urban, Suburban, and Rural Areas, NASA CR 72490 February 1969.
4. Mills, A. H.: Measurement of Radio Frequency Noise in Urban, Suburban and Rural Areas, NASA CR-72802, Dec. 1970.
5. Feasibility Study of Man-Made Radio Frequency Radiation Measurements from a 200-Mile Orbit, General Dynamics RZK 68-007, February 1968.
6. GSFC Specification RFI Receiver Performance, S-700-P1, Amended October 1971.
7. Technical Proposal for RFI Receiver, AIL Exhibit A to Proposal J-5407, July 1971.
8. Final Report: Improved Measurement Techniques for Spectral Power Output Data, RADC-TDR-63-469, Sept. 1963.
9. Spectrum Analysis, Hewlett-Packard Application Note 63, August 1968.

APPENDIX D  
DATA HANDLING



#### D. DATA HANDLING

The following subsections discuss, in general and for some specific examples the data flow, storage and processing associated with the man-made noise experiment. In order to create the most efficient data handling system the data storage and processing must be designed with both the receiver operation and ultimate experiment output in mind.

As previously discussed the overall objective of this experiment is to develop a data base that can be used for assessing the levels of man-made electromagnetic radiation or interference at satellite orbital altitudes. The approach to be used in this experiment to measure interference levels basically involves two modes of operation. The first mode and the one which will be used the majority of the time involves the measurement and storage of peak power levels as a function of frequency, geographical area, time of day and time of year and satellite altitude. The objective of this operational mode will be to develop power flux density maps that depict the levels of interference as a function of the above parameters. The second mode of operation is designed to measure interference levels in narrow frequency bands, over small geographical areas, at specific times of the day or year on a demand basis. If, for example, there is a requirement for the measurement of interference levels in a given narrow frequency range, say 2550-2690 MHz over a specific geographical area, say New York City, this experiment provides for operational procedures to allow for this type of

data collection. It is important to distinguish between these two modes of operation before discussing the data handling and processing procedures because the absolute resolution requirements for the stored data impact the data processing and storage portions of the experiment. As will be shown in the following section it is not practical and feasible to collect peak power data with a resolution of 20 kHz and a geographical resolution of a few feet and store this type of data for compiling power flux density maps over the entire 400 MHz to 12 GHz frequency range and the entire orbital sphere. However, for specific analysis and measurement of frequency bands at a given geographical location a geographical resolution of several hundred feet and a frequency resolution of 20 kHz would be desirable and is feasible.

The basic processing algorithms and data reduction procedures will be similar for both the "on demand" type measurement and the long term power flux density data collection. The primary difference between the two modes will be the difference in the resolution cell to be used in the data storage library.

#### D.1 General Data Library Requirements and Structure

The structure of the data library is determined by several factors:

- o It must contain the necessary information needed to generate power flux density maps and other interference statistics on the received man-made noise.

- o Its structure must allow the most efficient updating of stored data by adding new data as it is taken and
- o It should be a fixed predetermined size so that the physical number of storage tapes do not grow in an unbounded manner as the experiment progresses.

Beginning with the smallest portion of the library, the individual "frequency record" records and working outward, the structure of the library is as follows:

#### D.1.1 Frequency Record

The frequency record contains the actual information gathered about the received man-made noise. This information should include the basic sampling statistics of the recorded RFI data including a percentile breakdown of all of the received RFI data on the basis of the received power level. Since the dynamic range of the man-made noise receiver is approximately 70 dB the frequency record could contain ten percentile data blocks each data block containing the number of received samples falling within a specific 7 dB increment of the receiver's dynamic range. A finer power resolution is of course possible, however if the library is to be completely structured (i.e., fixed in size) at the onset of the experiment, then storage must be set aside for the maximum number of samples that could be expected to fall within any of the power increments. If for example it was felt that to be an accurate statistic each frequency record (i.e., at each specific frequency, geographic, time of day,

time of year and altitude data point) had to hold at least 1023 samples then each of the percentile data blocks must be allotted 10 bits within the frequency record to allow for the possibility of all 1023 samples falling within the same power range. If the dynamic range of the receiver is divided into 20 increments of 3.5 dB, instead of 10 increments of 7 dB, then the ultimate resolution of the distribution is more accurate but the data storage requirements are doubled unless the total number of samples required to produce an "accurate statistic" is reduced. These two factors do not trade-off linearly, however, since it requires 100 data bits to store 10 percentile blocks each holding a number from 0 to 1023 but 100 data bits holding 20 percentile data blocks (of 5 bits each) would allow only 31 samples to be stored in each.

In addition to storing percentile power statistics on the received man-made noise the maximum and the minimum power level record should also be stored. These words are stored in order to allow the rapid creation of accurate maximum and minimum power flux density maps.

The actual structure and size of an individual frequency record and therefore the information content of the record should be structured with the processing computer in mind. For example, the CDC 6600 uses a 60 bit word, 15 bit byte, so the smallest number of bits conveniently handled by the arithmetic sections of the computer (using assembly language) is 15 bits, while access to the core memory is performed in 60 bit units. A XDS

Sigma 7 on the other hand uses a 32 bit word with an eight bit byte. Obviously, the most efficient frequency record structure for the CDC 6600 would not operate efficiently on the XDS Sigma 7 computer.

#### D.1.2 Diurnal Blocks

In order to store information of the diurnal variation of the man-made noise, separate storage allocations must be available for each segment of the day in which the data is taken. One method of accomplishing this is to create several areas within a single frequency record, one for each diurnal period required. Each of these storage areas would contain the same number of bits (percentile power numbers, etc.) and would hold information on the RFI taken during a specific portion of the day. A second method of accomplishing this is to have several separate groups of frequency records, each group corresponding to a specific portion of the day.

The actual long-term data storage will be accomplished by using magnetic tapes. The information on a magnetic tape is most easily read into the computer in a sequential manner. This means that if a frequency record contained several diurnal blocks, all of the diurnal information associated with a specific frequency record will be read off of the tape whenever several frequency blocks are. Since the data received at the data processing center from the ground stations will be in the form of received data gathered on individual satellite passes, the incoming data will be processed in batches where the diurnal

variation of the data, in any single batch, is at most about 15 minutes, i.e., the longest satellite visibility period.

If the day is divided into relatively large segments, quarters for example, then any given batch of input data will most likely fall within a single diurnal period. This means that by storing the frequency records in groups according to the diurnal periods only a single group of frequency records must be read off the tape at any one time. So, placing the frequency records into groups where each group represents a specific portion of the day will reduce the core requirements of the data processing programs, making for a more efficient experiment data flow.

Several factors must be considered in determining the number of diurnal periods used in the data storage library.

- (1) It is quite possible that local time of passage for ascending (or descending) satellite passes near a single ground point will occur within the same 2 or 3 hour period every day for several months. This can happen even for a non-sun synchronous orbit. If data is to be taken for a specific frequency band continuously for a one to two month period, then all of the data taken would apply to only one or two diurnal blocks.
- (2) The diurnal resolution required for the experiment will probably be very gross, say morning, afternoon, evening and night. And finally, some frequency bands may show little or no diurnal variation.

### D.1.3 Geographic Bin

The man-made noise receiver is capable of generating one data word for every 10 feet, or so, of satellite movement. If the receiver is operating in the 10 MHz scan mode it can return to the same frequency after 500 data words or a little over one kilometer of satellite movement. If a ground resolution of 50 or 100 km is required in the data storage library then the data generated by the 10 or 15 seconds of receiver will apply to many frequency records but only one or two geographic bins (geo-bins). The most efficient method of structuring the library then is to have a complete set of frequency records and diurnal blocks within each geo-bin. With this structure several hundred or thousand consecutive data words will be processed into a contiguous area of library magnetic tapes. If the structure were reversed, that is storing geographic information within a frequency record then a new tape area would have to be accessed whenever the receiver produced a data word concerning a different frequency.

The method in which the earth's surface is broken up into geo-bins will also impact the efficiency of the data flow. On preliminary inspection it may seem reasonable to divide an area up strictly in terms of latitude and longitude lines, for example, a geo-bin could be chosen to be an area of  $1^{\circ} \times 1^{\circ}$ . However, while one degree of latitude remains fixed at about 111 km, one degree of longitude varies from 111 km at the equator to 0 km at the earth's poles. If each geo-bin is to contain the same geographic area then this method becomes very cumbersome. A second method might be to simply divide the earth's surface

into approximately square regions of equal area without regard to latitude and longitude. This method, while aesthetically pleasing because of nice square bin shapes doesn't consider the fact that the point at which a specific data point is taken is a function of the satellite's orbital parameters. Again, the magnetic tape is a sequential storage device and with this scheme there is no guarantee that when the satellite leaves the geo-bin it will automatically enter the next geo-bin on the library tape. This would mean a large amount of potentially unnecessary tape changes and tape scanning when the receiver data is processed into the storage library.

A third library structure, which overcomes the problems outlined above, would be to define two of the four borders of a geo-bin by actual satellite tracks spaced a specific number of longitude degrees apart at the equator and then, since the satellite tracks approach each other in distance (but not in degrees of longitude) as the satellite moves away from the equator define the remaining two bin boundaries by latitude lines spaced so as to keep the total surface area within any geo-bin constant. An example of this type of geo-bin is shown in Figure D-1. Each of the geo-bins shown in the figure has an areas equivalent to that of a square with 150 km sides.

There are a number of benefits arising from this type of geo-bin structure. If all of those geo-bins which lie between track 1 and track 2 of Figure D-1 are stored on the same magnetic tape and the bins are stored in order, starting at the equator and going to the maximum latitude that the subsatellite passes



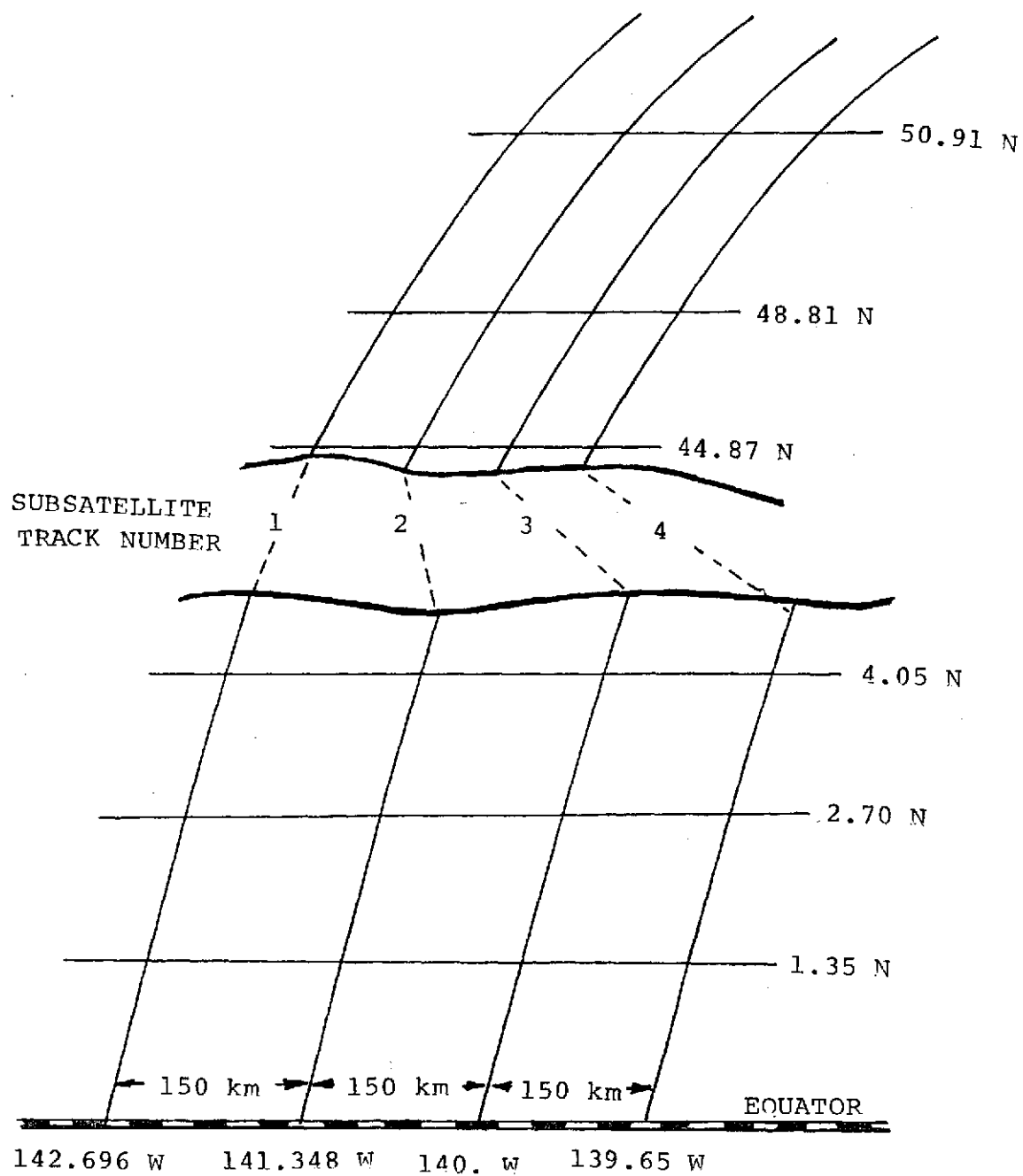


FIGURE D-1. EXAMPLE OF PROPOSED GEOGRAPH-BIN  
STRUCTURE.

over, then whenever the satellite crosses the equator ascending between longitude 141.348°W and 142.692°W all of the data generated by the receiver must pertain to that one storage tape. Also the geo-bins within that storage tape will be exercised in sequence so that only one pass of the storage tape is required for any pass of the satellite over a ground station. Two other benefits arise from this system, namely:

- (1) Since there is a direct relation between the equator crossing time and the time a satellite will cross any given latitude for a specific orbit, once the time of the commencement of data transmission is known it is very easy to relate a specific data position in the satellite data stream to a specific geo-bin, and
- (2) Geo-bins developed in this manner can be summed to produce larger geographic-bins very easily, with no overlapping of the geographic areas involved.

The equations required to produce these bin boundaries are very simple and are obtained as follows:

The area of a spherical ring located coaxially with the earth's rotational axis is given by

$$A_{\text{ring}} = 2 \pi R_e^2 (\sin L_2 - \sin L_1) \quad (1)$$

where:  $R_e$  is the average earth radius

$L_1$  is latitude of the lower edge of the ring

$L_2$  is the latitude of the upper edge of the ring

The portion of the ring lying between two orbital tracks "d" degrees apart is given by  $d/360$ , regardless of the shape of the orbital tracks. So if the required geo-bin area is given by  $A_{gb}$  then

$$A_{gb} = (d/360) 2\pi R_e^2 (\sin L_2 - \sin L_1) \quad (2)$$

The spacing of the orbital tracks can be obtained by letting the boundary spacing (in km) at the equator ( $L_1 = 0$ ) be equal to the side of a square whose area would equal  $A_{gb}$  and Equation (2) can then be solved for the latitude  $L_2$  required to make the bin area equal to  $A_{gb}$ . This latitude is:

$$L_2 = \text{ARCSIN} (\sqrt{A_{gb}}/R_e + \sin L_1) \quad (3)$$

This process is repeated resetting  $L_1$  to  $L_2$ , to obtain the next higher latitude bin boundary. Various modifications to this technique can be used to produce the "squarest" geo-bin at any desired latitude.

As an example, Table D-1 shows the latitude boundaries for bin areas of  $2.5 \times 10^5$  and  $10^6$  sq km (equivalent to squares with 500 and 1000 km sides respectively). Also shown in the Table are the verticle dimensions of each bin both in degrees of latitude and in km and the approximate time (in seconds from equator crossing) that a satellite in a 1000 km,  $63.5^\circ$  inclination orbit would enter a specific geo-bin. The forth column in Table D-1 (% increase vert) gives the percentage increase of the vertical dimension of the geo-bins as compared to the horizontal bin

TABLE D-1

EXAMPLE OF PROPOSED GEO-BIN STRUCTURE

INCLINATION (DEG), ALTITUDE (KM) 63.5, 1000

INITIAL GEO-BIN SIDE (KM) = 1000

GEO-BIN LENGTH INCL. = 2.9833 (DEG)

LAT	BIN VERT (DEG)	BIN INCREASE (KM)	TIME (SEC)
9.02	9.021	1004.1	0.00
18.27	9.254	1009.2	176.58
27.06	9.723	1019.0	358.96
38.14	10.722	1209.3	554.90
51.52	12.723	1422.5	772.59

INITIAL GEO-BIN SIDE (KM) = 500

GEO-BIN LENGTH INCL. = 4.4917 (DEG)

LAT	BIN VERT (DEG)	BIN INCREASE (KM)	TIME (SEC)
9.02	4.496	500.0	0.00
18.27	4.524	503.0	87.95
27.06	4.582	510.0	176.58
38.14	4.673	522.1	268.53
51.52	4.702	534.0	358.96
63.50	4.981	554.3	454.59
73.28	5.224	581.3	554.90
88.04	5.559	618.0	661.87
94.07	6.033	671.6	772.59
91.02	6.729	751.3	910.53
99.58	7.557	855.8	1076.35

REPRODUCIBILITY OF THE  
ORIGINAL PAGE IS POOR

dimension at the equator and is a measure of the elongation (latitudinal) and narrowing (longitudinal) of the bin shape caused by the two satellite tracks approaching each other in distance at the higher latitudes. As mentioned previously and as can be seen in the Table D-1 four of the  $2.5 \times 10^5$  geo-bins fit exactly into one of the  $10^6$  geo-bins. Figure D-2 shows the geo-bin shapes for  $10^6$  sq km bins superimposed over the visibility circle of the spacecraft as seen from GSFC/NTTF.

#### D.1.4 Altitude and Seasonal Sublibraries

Each receiver data word is also a function of the time of year it is taken and the orbital altitude at which it is taken. Perhaps the best way to structure the overall data library is to physically separate it into eight sections on the basis of altitudes near the apogee and perigee altitudes and the four seasons of the year.

While this seasonal division is extremely arbitrary, if a seasonal variation in man-made noise is to be looked for some allowance must be made in the data storage library for incorporating this parameter. Since the standard operation of the receiver will probably be to take data over a given frequency band for a period of at most a couple of months, only that portion of the library pertaining to the current season must be available at the data processing center. The remaining three quarters of the library could remain in a storage area that does not have to be physically located near the operations center.

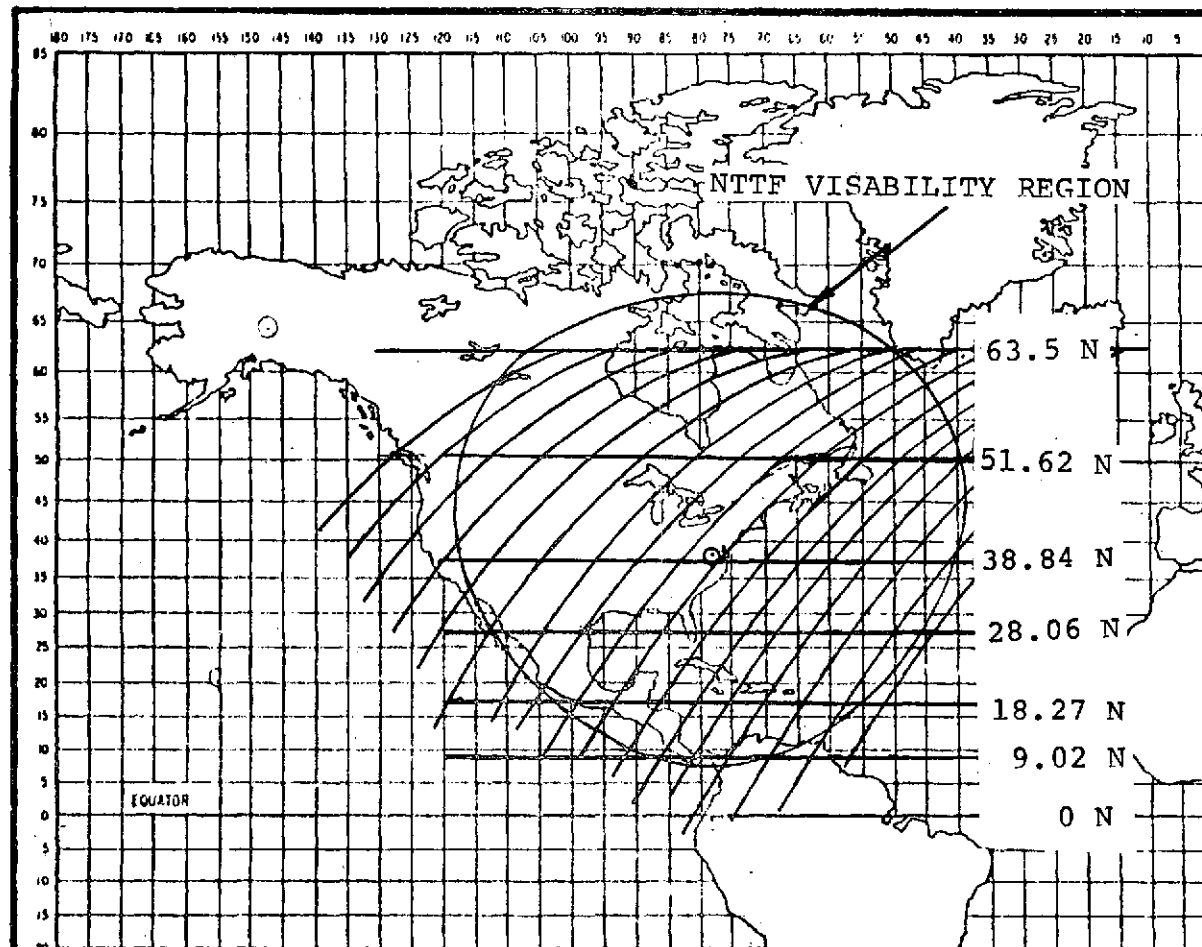


FIGURE D-2. EXAMPLE OF GEO-BIN STRUCTURE

Dividing the library in terms of satellite altitude is justified on the basis of efficient data processing. Since the taking of data by the man-made noise receiver will probably be restricted to altitudes within a set percentage of the apogee or perigee, a single satellite pass of a ground station will not contain data from both ascending and descending portions of the orbit. The processing of any given receiver generated data tape would access only one library tape in either of the two altitude libraries. Another and more important reason for segregating the altitude libraries is the structure of the geo-bins. Geo-bins set up for any single ascending pass will be contained on a single library tape and will be accessed in the sequence that they appear on the tape, a descending pass would cut across the geo-bin such that many library tapes would have to be accessed for any one pass. The most efficient method of structuring the storage library would be to have two separate sets of library tapes one for ascending passes and one for descending passes, each of which has its own geo-bin structure.

#### D.1.5 Data Storage Library Structure Summary

Each data word generated by the man-made noise experimenter is actually a function of five variables:

- o Frequency
- o Geographic Position
- o Time of Day

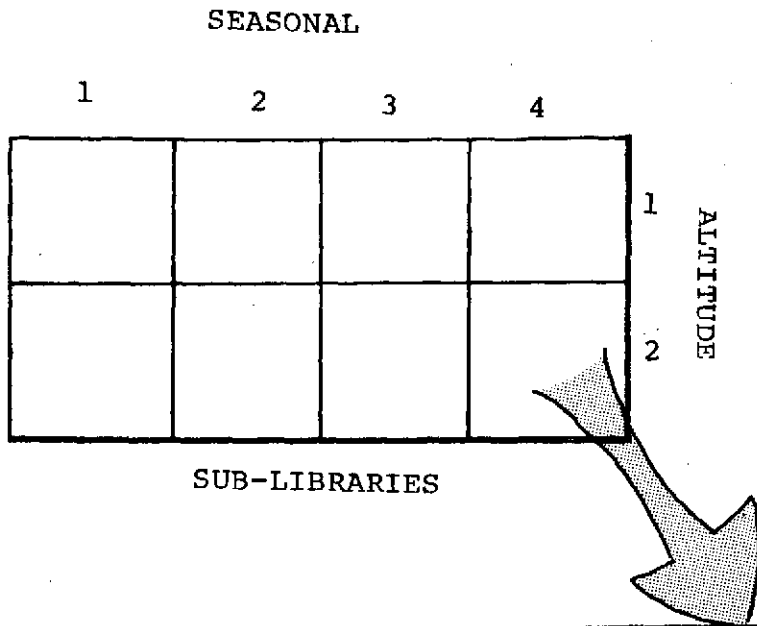
- o Time of Year
- o Spacecraft Altitude

The structure of the data storage library must take all five of these variables into account and yet must allow for the fastest most efficient operation, utilizing sequential magnetic tape storage.

Figure D-3 shows, schematically, the proposed library structure. The library is physically divided into eight separate sublibraries of storage tapes, only two of which (both altitude sublibraries for any one season of the year) must be accessible to the data processing center at any given time.

Each sublibrary consists of a fixed number of magnetic tapes, only one of which is required to process the receiver generated data for any single satellite pass of a ground station. The information on each tape is initially divided in geographic regions (geo-bins) each of which will be accessed sequentially during a data processing operation. Each geo-bin is divided into several diurnal blocks, only one of which is used for a single updating of the storage data and finally each diurnal block is divided into a series of frequency records. Each frequency record will be accessed sequentially for an updating operation and contains statistically information concerning the man-made noise received in a specific frequency increment, at a specific time of day, within a specific geographic area, within a specific altitude range and in a given season of the year.





GEO-BIN No. 428

DIURNAL BLOCK No. 1

FREQUENCY RECORD No. 1  
 FREQUENCY RECORD No. 2  
 FREQUENCY RECORD No. 3

DIURNAL BLOCK No. 2

FREQUENCY RECORD No. 1  
 FREQUENCY RECORD No. 2

GEO-BIN No. 429

FIGURE D-3. LIBRARY STRUCTURE

## D.2 Data Volume Impact on Experiment

If properly structured, the total volume of the data storage library will not be a function of the total number of data samples produced by the man-made noise receiver. Since information is actually stored in the form of statistics concerning the received data, each new piece of data merely modifies the statistics and does not actually increase the size of the overall storage requirements.\*

However, each set of statistics contained in the data storage library is actually a function of five parameters and the way these parameters are broken down very greatly impacts the overall size of the library.

For example, if an attempt were made to store all of the man-made noise data at the following resolutions:

Geographic resolution	10 km
Frequency resolution	20 kHz
Diurnal resolution	4 quarters of the day
Seasonal resolution	4 seasons of the year
Altitude resolution	2 altitudes

and three computer words (180 bits) were required to store the information on each data statistic, then over 87,000,000 individual magnetic tapes would be required. Table D-2 shows how this value is arrived at.

\* Note, This statement is true as long as the number of data samples falling into a single percentile slot is below a pre selected number. The actual selection of the value is considered later in the report.

TABLE D-2

STORAGE REQUIREMENTS FOR HIGH RESOLUTION,  
COMPLETE DATA STORAGE LIBRARY

Seasonal Sublibraries	4
Altitude Sublibraries	2
Geo-Bins	
= Total Longitude x Total Latitude / Bin Area (368)                    (135°)    (.01°)	$4.68 \times 10^6$
Diurnal Blocks	4
Frequency Records	
= Total Frequency Band / Frequency Increment (12x10 <sup>9</sup> )                    (2x10 <sup>4</sup> )	$6 \times 10^5$
Total No. of Frequency Records	$8.99 \times 10^{13}$
Bits per Frequency Record	<u>180</u>
Total No. of Bits to be Stored	$1.62 \times 10^{16}$
Bits per Storage Tape*	<u><math>1.87 \times 10^8</math></u>
Total Number of Tapes Required	$8.7 \times 10^7$

\*One 2400 ft., 9 track, 800 bpi tape at 90% packing efficiency can store  $1.62 \times 10^{16}$  bits

Obviously, it would be impractical, if not physically impossible\* to attempt to utilize a data base of this size.

Inspection of Table 4-2 shows that there are three major parameters which may be varied to reduce the size of the data library: the size of the geographic resolution element, the size of the frequency resolution element and the number of bits included in a single frequency record. In addition if either the total geographic area or the total frequency bandwidth to be stored in the library is reduced, then the total volume of the library is reduced. The following sections deals with practical methods of increasing the geographic and frequency resolution element, and thereby decreasing the data processing burden and storage. The following section discusses the effect that varying the above parameters has on the size of a practical data storage library.

#### D.2.1 Methods of Reducing Data Volume

Because of the large range of potential uses that exist for the receiver, it has been designed to gather information in very fine frequency and geographic increments. Some of the experiment objectives, however, do not require 20 kHz frequency resolutions or 3 ft. geographic resolution and, as just discussed, any attempt to create a general data base to contain RFI data covering the entire frequency and geographic ranges covered by the receiver at the maximum resolution that

\* $87 \times 10^6$  tapes would require a one story building with about 700,000 sq. ft. of floor area, not counting passage ways.

the receiver is capable of seeing leads to a prohibitably large data tape library. For these reasons the experiment has been designed such that either or both the frequency resolution and the geographic resolution may be decreased. This decreased resolution will decrease the experimental data flow volume and total data library requirements and subsequently decrease the data processing and handling time and cost. Those applications requiring the full resolution requirements, may, of course, restrict other system parameters such as the total geographic area or the total frequency band over which data is taken, in order to control the data library size and processing load.

#### D.2.1.1 Frequency Resolution

The ultimate frequency resolution of the AAFE receiver is the bandpass of the last predetection filter. The receiver outputs one seven bit peak amplitude word for each 20 kHz frequency band. The frequency resolution may be decreased by considering groups of frequency/peak-amplitude words and choosing the one with the largest value. If, for example, the experiment output were to be in the form of PFD maps generated for every 100 kHz of the RF spectrum, five of the receiver output amplitude values would be combined, reducing the quantity of data by a factor of five.

In order to obtain the greatest savings in data handling, this data summation process should be implemented as close to the data source as possible. And since some special ground station interface equipment is required, the addition of this summation capability would not significantly increase the special equipment complexity.

#### D.2.1.2 Geographic Resolution

The second variable resolution parameter is the geographical coverage during a single frequency detection period. In the single frequency mode, the receiver is designed to operate at a maximum data output rate of one data word every 100  $\mu$ sec and to return to the same 20 kHz frequency slot every 500  $\mu$ sec. During this 500  $\mu$ sec the spacecraft subsatellite point will travel approximately 3 meters. The receiver has been designed so that distance between samples at the same frequency may be increased by slowing down the CDSC data request clock. If the experiment operator felt that a distance between data/word at each frequency of 300m were sufficient he could reduce the onboard data clock by a factor of 100 by ground command, and he would simultaneously be reducing the experiment data flow and data storage requirements by two orders of magnitude.

#### D.2.2 Sizing the Data Storage Library

This section discusses the trade-offs involved in designing a practical data storage library.

#### D.2.2.1 Frequency vs. Geographic Resolution

The input data consists of multidimensional amplitude (7 bit) words. Multidimensional in the fact that each amplitude data word is a function of five variables.

For most purposes, some of the parameters can be broken into very coarse increments e.g., time of year - 4 parts (seasonal); time of day - 4 parts, altitude - 2 altitudes.

The frequency and geographic parameters associated with a specific amplitude word are actually ranges and not specific numbers, that is the receiver's minimum bandwidth or frequency resolution is 20 kHz and since the detector is of the peak-hold and reset type the amplitude word corresponds to the maximum value of RFI received while the spacecraft sub-satellite point moved approximately 3 ft.

If each of these 8 separate sublibraries (4 seasonal x 2 altitude) is limited in the number of tapes it may contain, the following paragraphs will yield an idea of how total tape volume constraints will effect the frequency and geographic resolution of the data base.

Each tape may contain approximately  $1.87 \times 10^8$  bits, if each record consists of 180 bits, each tape can therefore hold about  $1.04 \times 10^6$  records where each record contains information about a single frequency bin, a single geographic bin and a single time of day bin.

Since there are 4 time of day bins this leaves 259,200 frequency and geographic bins per tape and if each of the 8 libraries is constrained to the following numbers of tape then the total number of available records is:

<u># Tapes</u>	<u># Records</u>
5	1,296,000
15	3,888,000
20	5,184,000
25	6,480,000
50	13,960,000

Instead of considering the entire orbital sphere look at the data which can be collected from a single ground station in real time.

- The ground radius from the ground station to the satellite (5° above the horizon, 1330 km altitude) is 3280 km. The total surface of the earth encompasses in the visibility circle of the ground station-satellite system is  $33.097 \times 10^6 \text{ km}^2$  breaking this into equi-area geographic bins implies

$$(1) \quad N_g = \frac{33.097 \times 10^6}{R_g^2}$$

$N_g$  = number of geo-bins

$R_g^2$  = area of a geo-bin (km)



Figure D-4 shows this relation.

Notice that even if 25 tapes were used and the data base was to contain information on the entire receivable frequency spectrum ( $12 \times 10^9$  Hz) then an obscrdly gross ground resolution of 500 km (133 total geo-bins) would require each frequency bin to be greater than 245 kHz.

The largest contiguous set of space frequency allocation cover 800 MHz (from 3.4 GHz to 4.2 GHz) so it might be reasonable to limit the operational mode of the receiver to bands 800 MHz wide. Another breakpoint may be to limit the receiver to 1 GHz. This would mean taking sufficient data to define a 1 GHz or 800 MHz portion of the spectrum, process the data bank and either store it at some facility away from the processing center or just destroy it and reuse the tapes.

Since the receiver range is 0.4 GHz to 12.4 GHz, suppose the receiver operation and data bank are divided into 12 - 1 GHz ranges. The total number of frequency bins ( $N_f$ ) required for each 1 GHz range is given by

$$(2) \quad N_f = 10^9 / R_f \quad \text{where } R_f \text{ is the frequency bin width (Hz) or frequency resolution}$$

Combining Equations (1) and (2),

$$N_f N_g = \frac{33.097 \times 10^6}{R_g^2} \cdot \frac{10^9}{R_f} = \frac{33.097 \times 10^{15}}{R_g^2 R_f} \quad (3)$$

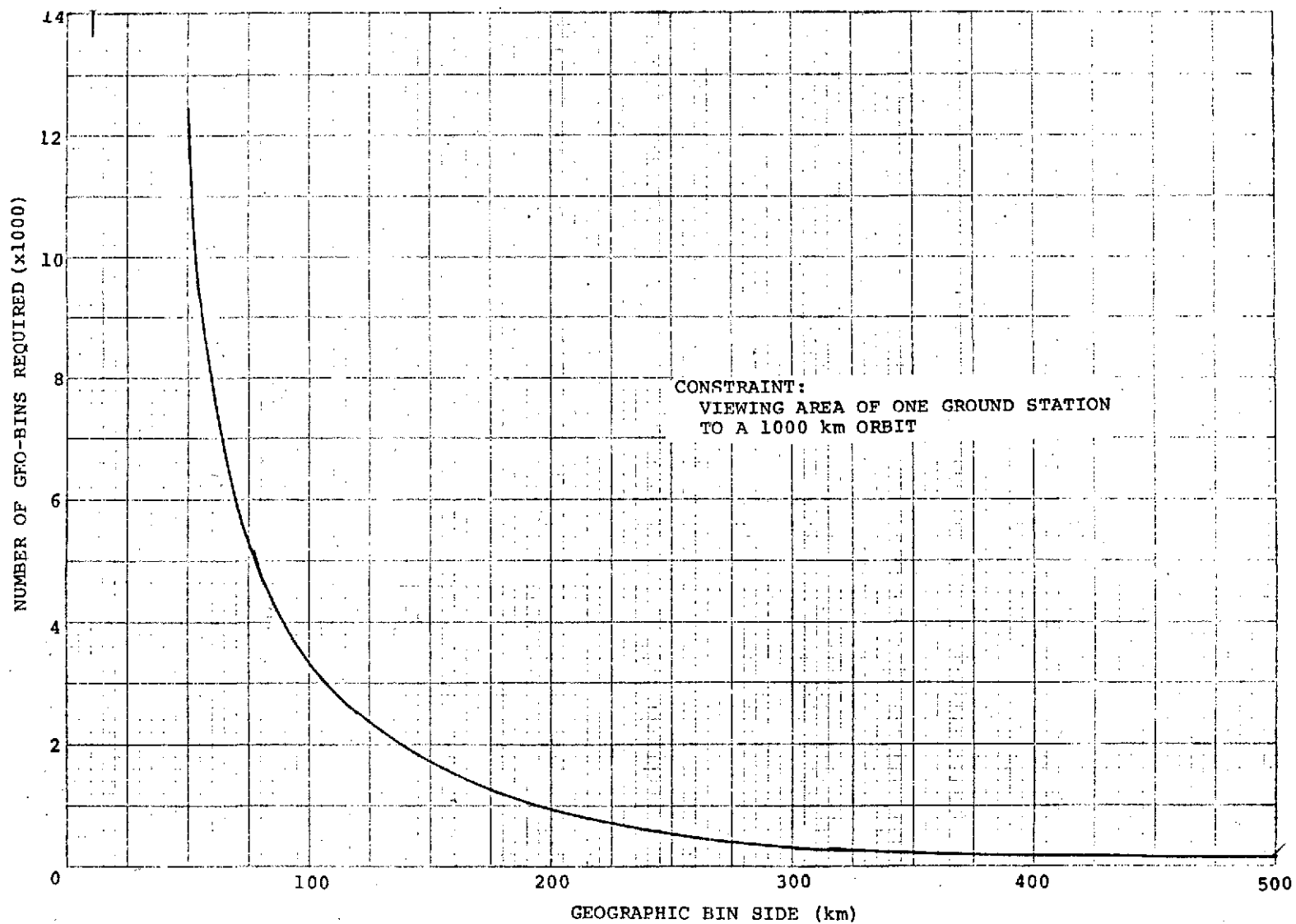


FIGURE D-4 GEOGRAPHIC BIN SIDE VS. NUMBER OF BINS REQUIRED

NATIONAL SCIENTIFIC LABORATORIES, WASHINGTON, D. C.

yields. Since  $N_f N_g$  is fixed by the total number of tapes available in which to store the data a parametric trade-off between frequency resolution and geographic resolution may be performed. Figure D-5 shows this trade-off for the previously given numbers of tapes.

It must be remembered that this is only one of eight sub-libraries being used by the experiment, so the total tape storage requirements of the entire program will be larger unless, all of the required information is extracted from the data bank on a seasonal basis and the tapes reused.

#### D.2.2.2 Frequency Record Size Considerations

As previously mentioned, the frequency record will contain statistical information in addition to the actual maximum and minimum values of man-made noise received by the experiment. There are 3 principal considerations in deciding how large a specific frequency record must be:

- (1) The number of samples required to produce a "good statistic";
- (2) the rate at which data will be collected which effects a particular frequency record and
- (3) compatibility of the record size with the processing computer.

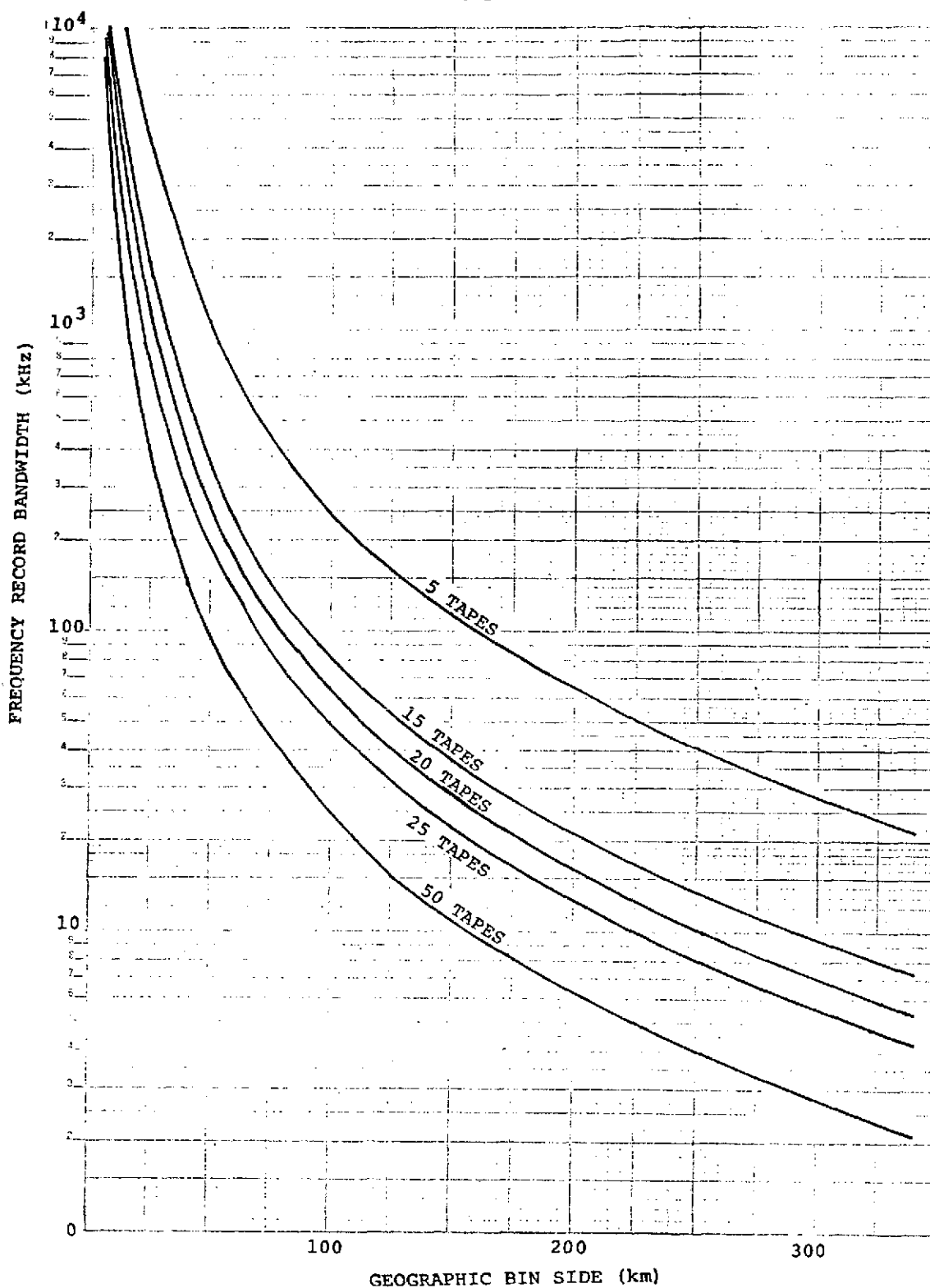


FIGURE D-5 GEOERAPHIC BIN SIZE VS. FREQUENCY RESOLUTION

The number of samples required to produce a statistically valid data set can be determined as follows: A method of constructing intervals which have a specified chance of covering a certain portion of a given population is based on the concept of tolerance interval. By way of definition, tolerance intervals are two numbers,  $X_1$  and  $X_2$ , such that one can make the statement that 70 percent (say) of the total population is contained between  $X_1$  and  $X_2$  with a confidence of 90 percent (say). The following table\* gives sample sizes required for various coverings and confidences.

TABLE D-3  
SAMPLE SIZE FOR TOLERANCE LIMITS

CHANCE OF COVERING STATED PROPORTION	PROPORTION OF POPULATION TO BE CONTAINED BETWEEN EXTREME VALUES OF A SAMPLE SET			
	.50	.90	.95	.99
.90	7	38	79	410
.95	8	47	97	490
.99	11	66	135	690

The above table was calculated by non-parametric methods and will apply for any distribution that is being sampled. If the form of the distribution is known, of course sharper statements can be made. However, if nothing is known about the distribution then the above table will define the number of individual samples required to cover a certain percentage of the unknown population with a certain confidence.

\*Dixon & Massey "Introduction to Statistical Analysis", 2nd Edition McGraw Hill, 1957.

For the man-made noise experiment then a good sample size should be, say greater than 690 samples, giving better than a 99% chance that the minimum and maximum power levels cover 99% of the power levels ever seen at specific frequency/geographic point, assuming no change in the ground population.

An estimate of the rate at which data will be collected in a specific frequency record can be obtained by looking at the satellite motion with respect to the geographical-bin size and the receiver data output rate. The receiver must either operate in a fixed frequency mode or a scanning frequency mode. If it is scanned, the minimum dispersion is 10 MHz. Since it scans the entire 10 MHz in .05 seconds, the receiver will return to the same frequency interval once every 0.05 seconds. During this time the spacecraft is moving 7.0 km/sec on the orbital sphere or its subsatellite point is moving about 6.0 km/sec across the surface of the earth. This means that the receiver is producing an amplitude word describing the same frequency at a minimum geographic separation along the subsatellite track of 300 m. As discussed before the raw data will be stored according to the geographic bin in which the subsatellite point resided when the data was taken. The range of this bin will probably be an area equivalent to a square with a side ranging from 50 to 300 km (i.e.,  $\sim 0.5$  to  $6^\circ$  at the equator) If, to obtain an upper bound, the satellite is moving diagonally across a square bin then the maximum number of samples taken at the same

frequency which can be taken in the same geographic bin is given by

$$\text{Max No Samples} = \sqrt{2} (\text{bin side}) / 300$$

Over an extended period the satellite track will return to the same geographic bin. From Table 3 section 2 of the Phase I report, the satellite track will repeat itself to within certain distance after a specific number of days or orbits. While the specific exact values of this cycle will not be known until the satellite is in orbit, the values given in the Phase I report (converted to km and shown in Figure D-6) will give "ball park" values.

The value of maximum samples per day for a given frequency-geographic point, as a function of geographic-bin size can be obtained by combining Equation 4 and Figure D-6 by assuming that data will be taken in the same geographic bin when even the satellite track repeats itself to within the geographic bin side length. This relation is shown in Figure D-7.

Compatibility with the processing machine is basically a function of the total number of bits contained in a record and how information is distributed within the bit grouping. For example, since the CDC 6600 utilizes 60 bit word, the number of bits in a single frequency record should be a multiple of 60 and since it uses a 15 bit byte (character) the most efficient organization from the machine viewpoint is to have 15 bits in a data word.

SCALE: 1 INCH = 1000 KILOMETERS  
 1 INCH = 100 KILOMETERS

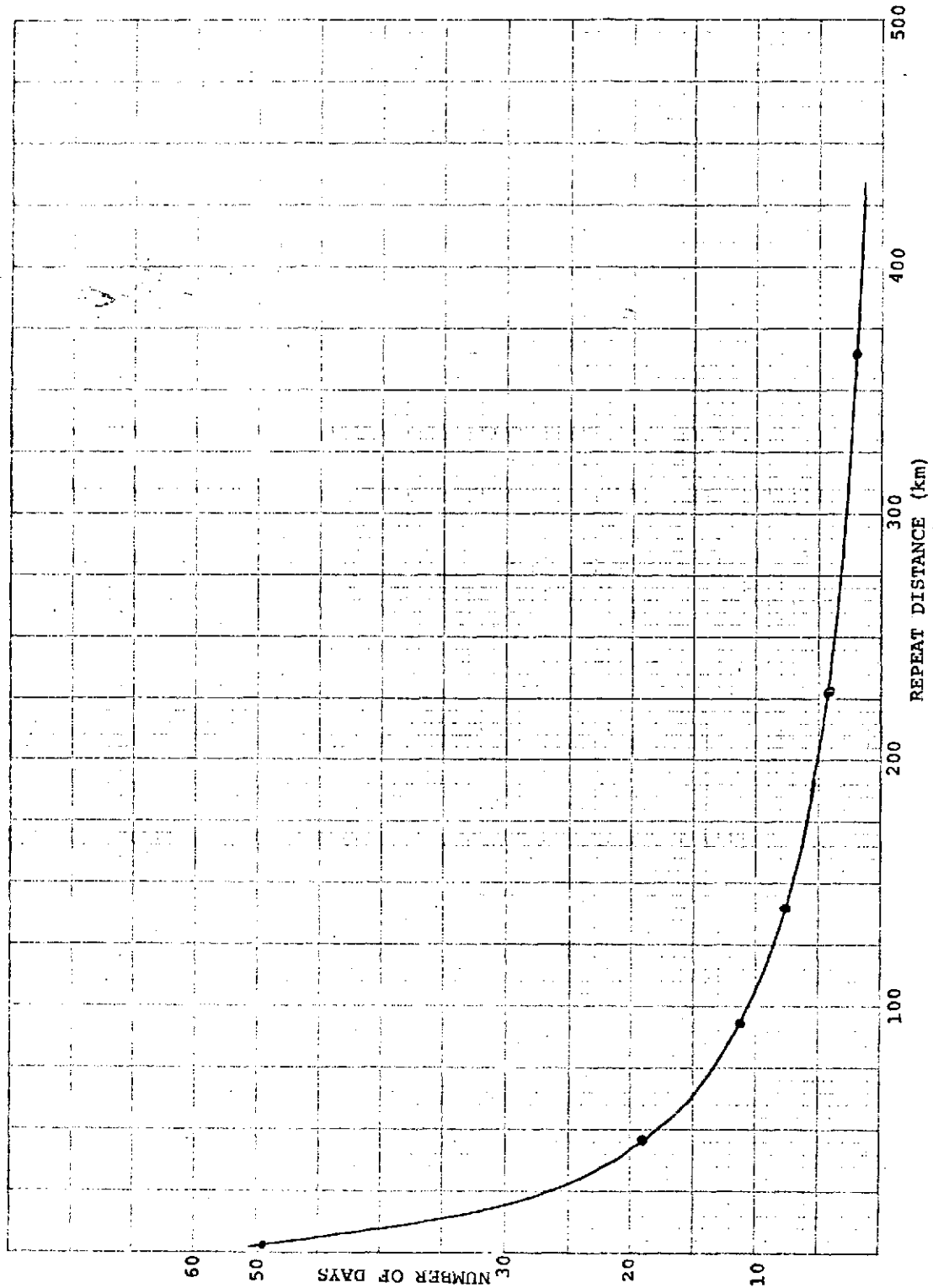


FIGURE D-6 SATELLITE REPEAT DISTANCE VS. TIME



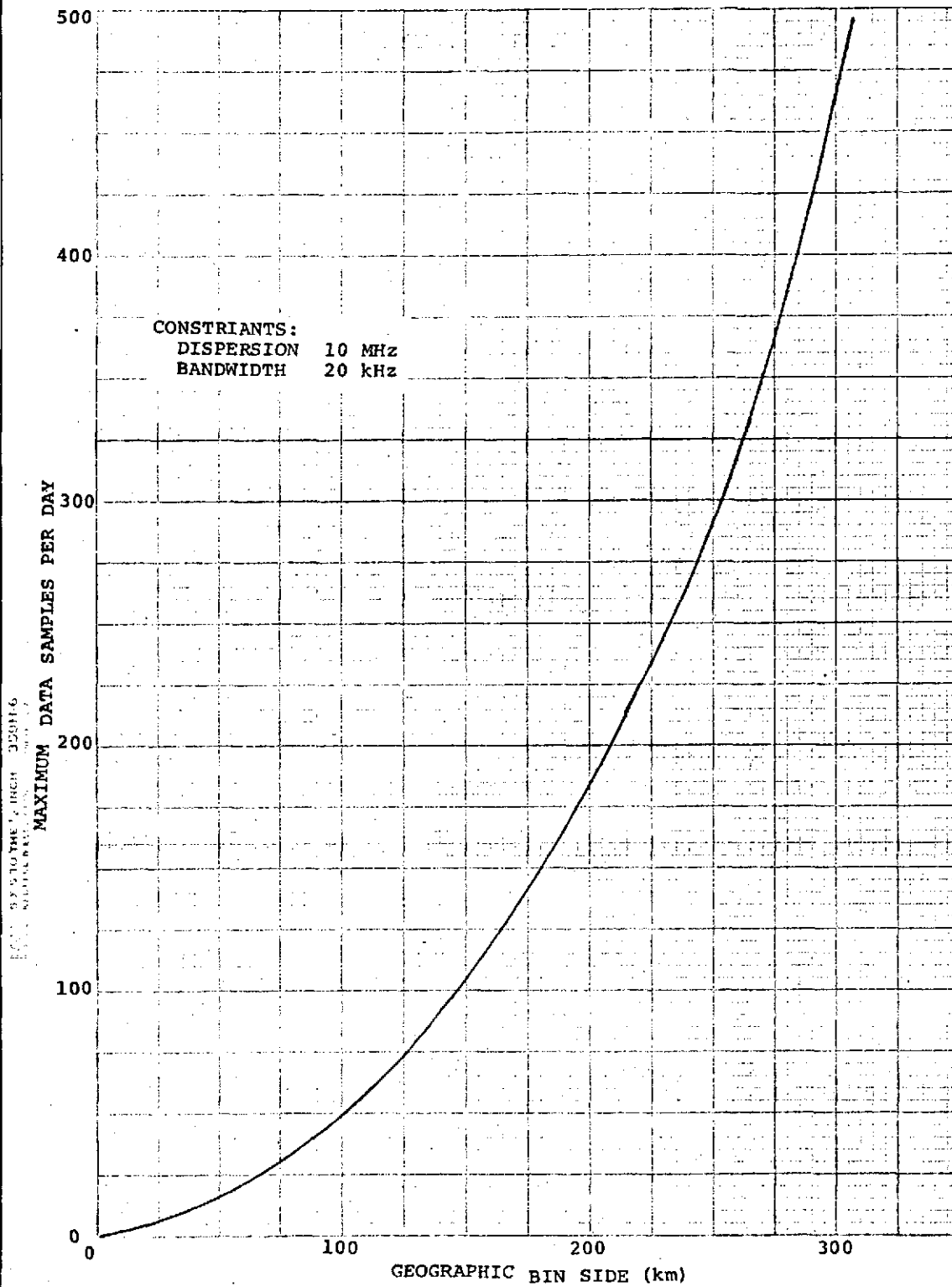


FIGURE D-7 MAXIMUM DATA RATE VS. GEO-BIN SIZE

While other frequency record structures are certainly possible, an example structure for the man-made noise experiment is as follows. Each record would consist of three CDC 6600 (60 bit) words (180 bits) and would contain 10-15 bit bytes holding percentile information on the recorded data. An eleventh byte will contain two 7 bit data groups indicating the maximum and minimum power levels recorded by the receiver for that record. The 15th bit of this word will be an overflow indicator that will be equal to 1 if any of the percentile bins is full. The final byte would be a frequency/diurnal indicator required to ensure that the proper frequency/diurnal data is processed into the frequency record. The structure of this record is shown in Figure D-8.

Each of the percentile bins would hold the number of recorded data samples falling within a 7 dB increment of the man-made noise receiver. Since each percentile bin contains 15 bits the largest number it can hold is  $20383_{10}$ . This is several orders of magnitude greater than the number of samples required to yield a valid set of statistics. However, from Figure D-7 if a large geo-bin is used then in two months of operation it could conceivably produce over 12,000 samples, a number which also requires 15 binary bits of storage. If any of these percentile bins is filled then the flag in Word 1, byte 2 is set up to 1 and no more data will be taken in the frequency record. At this point enough data will have been gathered to obtain a good idea of what has happened at this frequency-geographic point.

WORD

BYTE

	1	2	3	4
1	FREQ/DIURNAL IDENT	MAX	MIN	PERCENTIAL BIN No.1
				No.2
2	No.3	No.4	No.5	No.6
3	No.7	No.8	No.9	No.10

FILLED  
FLAG

FIGURE D-8. FREQUENCY RECORD

The frequency-diurnal byte (word 1, byte 1) will hold a binary word of up to  $20383_{10}$  which will indicate the exact frequency-diurnal record or the relative position of the particular record with respect to the near by records depending on how many frequency records are contained within a geo-bin.

#### 4.2.3 Sizing the Data Storage Library and Other Experiment Parameter

The information in the preceding sections may be used to obtain an estimate of the overall library size for a specific mode of operation of the experiment.

If, for example, the principle experiment decided that power flux density maps covering the U.S. were required for 2 GHz of the E-M spectrum and that two years of operation would be allotted to gather the required data.

If information is to be taken at 2 altitudes, ignoring seasonal and diurnal variation, then from Table D-3 the experiment must collect  $690 \times 2 = 1380$  data samples on each geographic/frequency resolution element in order to produce a good statistical basis for producing the PFD maps.

If the experiment is broken up into two portions, each collecting data on a 1 GHz spectrum, then 365 days will be allotted to gathering each part and the experiment must gather  $1385/365 \approx 4$  samples per day from each geographic/frequency

bin. Figure D-7 is based on a 10 MHz scan operate and only ascending passes, so if the receiver is actually scanning 1 GHz and collects both ascending and descending pass information, then the curve of average samples gathered per day vs. geographic bin size must be reduced by a factor of  $\frac{1}{2}$  ( $10 \times 10^6 / 10^9$ ) = 50. Therefore, a minimum geographic resolution element of about 200 km (on a side) must be used. Figure D-5 indicates that by using a 30 to 35 tape library, data may be gathered with a frequency resolution of about 100 KHz.

Since data on two different altitudes is to be taken, two sublibraries will be required and the total data tape requirements will be between 60 and 70 tapes for a 1 GHz portion of the spectrum.

It should be noted that at 100 kHz resolution it would require 10,000 PFD maps to cover 1 GHz of spectrum.

### D.3 Data Flow

The overall experiment data flow is shown in Figure D-9. The experiment generated man-made noise data is received by the ground station and forwarded to the central data processing station. At the data processing station two major types of operations are performed; updating of the data storage library and interpretation processing.

Updating of the data storage library requires inputs in the form of "raw" experiment data and principle experiment instruction, and consists of including the freshly taken man-made noise

REPRODUCIBILITY OF THE  
ORIGINAL PAGE IS POOR

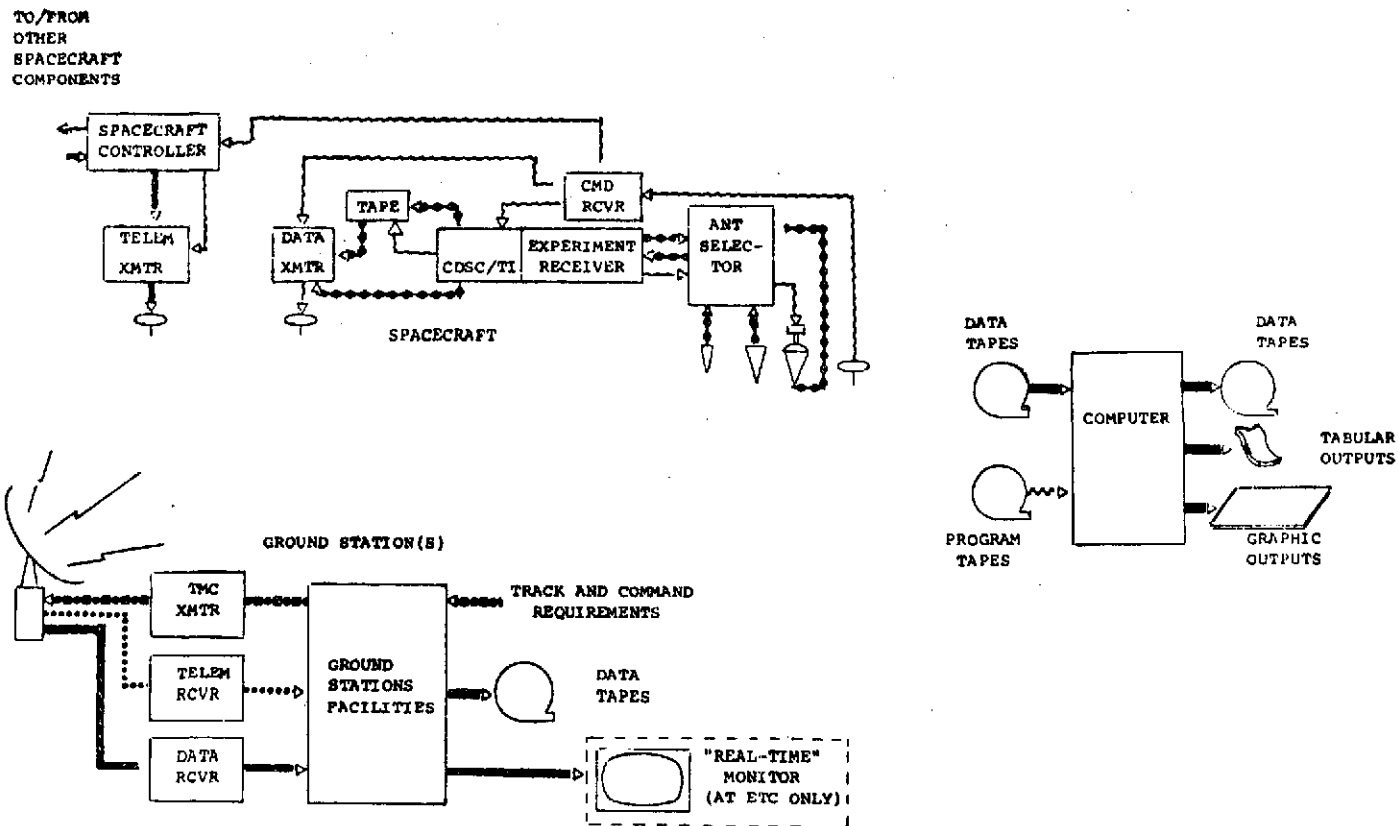


FIGURE D-9 OVERALL EXPERIMENT DATA FLOW

data samples in statistical data maintained in the data storage library.

Once sufficient data is collected to permit interpretation processing, the data storage library will be exercised, yielding the required experiment outputs in the form chosen by the principal investigator. These outputs may take the form of power flux density maps, statistical data on RFI diurnal variations or other.

The principal investigator defines the operational mode of the experiment and therefore construes the frequency coverage, antenna used and other parameters. These parameters along with orbital information and clock and calibration information are required in the updating of the data storage library.

The principal investigator is also responsible for the short and long range operational planning of the experiment. Among other items he must decide which frequency regions deserve detailed analyses, the best way the data output should be presented and in general how best to utilize the experiment. In order to assist the principal investigator in his decision making a "quick look" capability will be provided at one ground station, preferably the operational ground station nearest the data processing center (i.e, ETC, Greenbelt, Md).

### D.3.1 Updating the Data Storage Library

Figure D-10 shows the first level flow diagram used in inputting raw MMN data into the data storage library. As envisioned the updating process would proceed as follows.

The following instructions supplied by the principal investigator the computer operator would mount three data tapes, the data input tape, one data storage tape from the data storage library and a third blank tape. The program would initially check the information contained in an operators file (entered according to the experimenter instructions by the computer operator), the header information on the data storage tape and the first control block on the raw data tape. These three sources of information must agree before any information is changed in the data storage tape.

As discussed previously the structure of the information on any data storage tape is such that raw data can be processed and stored data modified in a sequential manner. The first processing operation after making sure that the proper data tape is being used with the proper storage tape is to determine where the applicable information resides on the storage tape. After the addressing of information on the storage tape is determined a block of raw data is read into the computer, converted to a statistical sample format and combined with the appropriate statistical data from the storage tape. These newly updated statistical data are then written out on the blank tape.



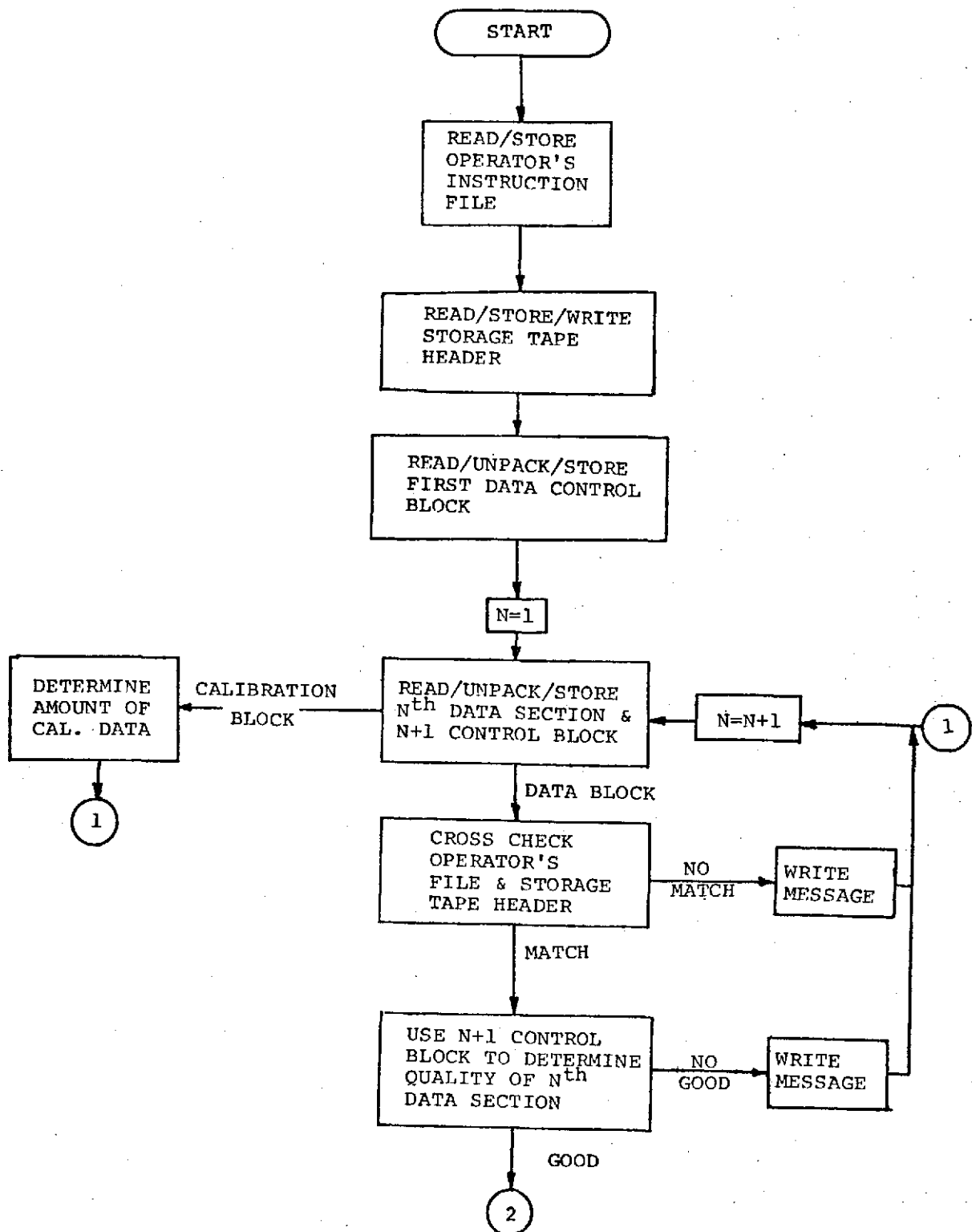


FIGURE D-10 FIRST LEVEL FLOW DIAGRAM

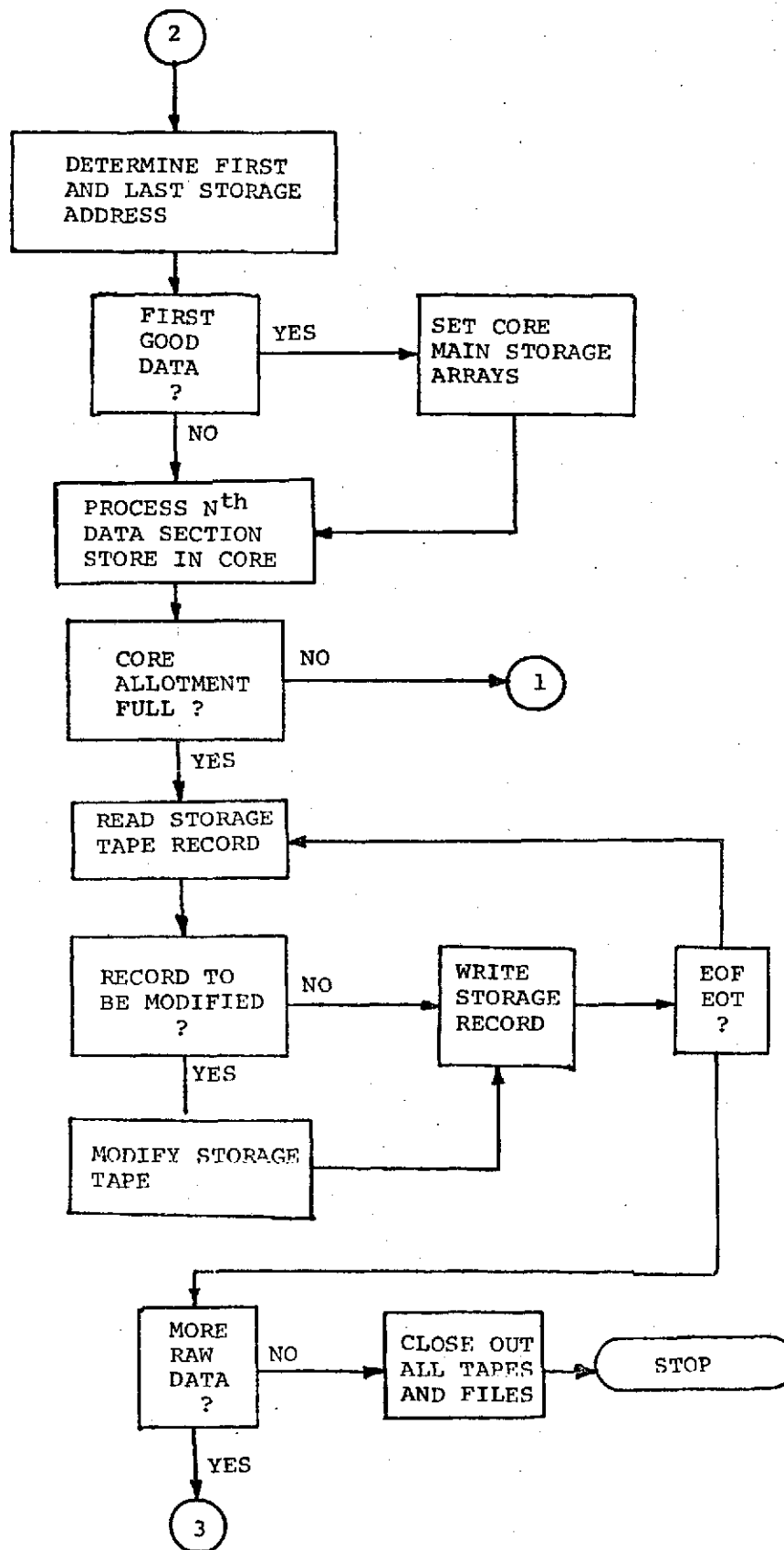


FIGURE D-10 (cont)

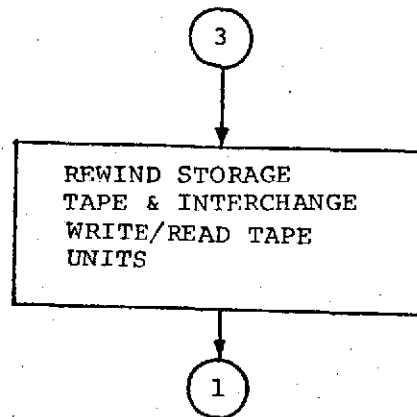


FIGURE D-10 (cont)

At the end of the updating process the old data tape and storage tape may be discarded or reused and the new storage tape returned to the data storage library.

#### D.4 GROUND INTERFACE EQUIPMENT

Because of the large range of potential uses that exist for the receiver, it has been designed to gather information in very fine frequency and geographic increments. Some of the experiment objectives, however, do not require finally detailed resolution and as discussed later any attempt to create a general data base to contain RFI data covering the entire frequency and geographic ranges covered by the receiver at the maximum resolution that the receiver is capable of seeing leads to a prohibitively large data tape library. For these reasons the experiment has been designed such that either or both the frequency resolution and the geographic resolution may be decreased. This decreased resolution will decrease the experimental data flow volume and total data library requirements and subsequently decrease the data processing and handling time and cost. Those applications requiring the full resolution requirements, may, of course, restrict other system parameters such as the total geographic area or the total frequency band over which data is taken, in order to control the data library size and processing load.

One of the variable resolution parameters is the geographical coverage during a single frequency detection period. In the single frequency mode, the receiver is designed to operate at a maximum data output rate of one data word every 100  $\mu$ sec. During this 500  $\mu$ sec the spacecraft subsatellite point will travel approximately 3 meters. The receiver has been designed so that distance between samples at the same frequency may be increased

by slowing down the CDSC word frame signal. If the experiment operator felt that a distance between data/word at each frequency of 300m were sufficient he could reduce the onboard data clock by a factor of 100 by ground command, and he would simultaneously be reducing the experiment data flow and data storage requirements by two orders of magnitude. (It must be noted that this command capability is not incorporated in the demonstration hardware command structure but can be obtained through external control over the word frame signal rate).

The second variable element is the ultimate frequency resolution of the AAFE receiver. The receiver outputs one seven bit peak amplitude word for each 20 kHz frequency band. The frequency resolution may be decreased (effective bandwidth increased) by considering groups of frequency/peak-amplitude words and choosing the one with the largest value. If, for example, the experiment output were to be in the form of PFD maps generated for every 100 kHz of the RF spectrum, five of the receiver output amplitude values would be combined, reducing the quantity of data by a factor of five.

In order to obtain the greatest savings in data handling, this data summation process should be implemented as close to the data source as possible. And since some special ground station interface equipment is required, the addition of this summation capability would not significantly increase the special equipment complexity.

The proposed ground interface equipment is shown in Figure 7-1. There are at least two manual inputs in addition to the man-made noise data. The input labeled "B" is the effective bandwidth of the spaceborne receiver and is a measure of the satellite clock setting being used in the MMN receiver. The interface equipment must have this information in order to "lock-onto" the incoming data stream. The second input labeled "N", is the number of data samples which are to be combined by the interface equipment. A description of the various components of Figure 7-1 follows:

VCO - the receiving flywheel - initially set (B) to the approximate S/C output data rate including doppler and is kept "locked" to the data rate by looking for transistions in the data.

Timing Gate/Transition Detection - Flywheel control - The timing gate is opened and closed at a specific interval around the time a data transition is expected. The transition detector looks for the specific time of the transition with respect to the center of the time gate. The VCO is adjusted to maintain the transition in the center of the gate limits. Since the S/C uses NRZ coding a transition will not occur every time.

Shift Register - Once the "flywheel"\* is locked onto the incoming data stream, the data is input serially into the shift register and advanced through the shift register. A comparator checks the binary data contained in the register for matches to one of the three system flags,  $F_1$ ,  $F_2$ , or  $F_3$ .

When  $F_1$  is found the next 56 bits (control block) are passed onto the data tape along with  $F_1$ . The logic then inhibits the transfer of data as long as  $F_3$  appears. After the last  $F_3$  flag, 500 (10,000 in fixed frequency mode) data words are passed on. If the  $F_2$  flag does not appear in its proper place, bits have been added or dropped from the data stream and an error code is written on the tape indicating that the previous data is invalid. If  $F_2$  is in its proper place the frequency words "NRTF" is passed onto the tape. If an  $F_3$  follows the NRTF the system idles, as before, until data begins appearing in the comparator. This process is continued until the  $F_1$  flag reappears starting the processes over again.

Peak Comparator - When data is to be transferred to the tape, the capability exists of combining several (N) of the frequency amplitude words, in order to reduce the data output. This reduction is accomplished by the second comparator (N must be preset before acquisition). This comparator chooses the largest of the N-7 bit words to pass onto the parity formatter logic. The tape format chosen for the experiment should be made to facilitate later data processing.



APPENDIX E  
THRESHOLD MEASUREMENTS

## I. AVERAGE SIGNAL POWER DETECTION

### E.1.0 MODEL

The model of this detection problem is shown in Figure E-1 in block diagram form:

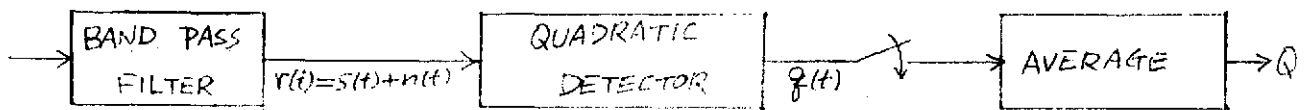


FIGURE E-1 Block Diagram

The received signal plus noise is band limited by the band pass filter. The output  $r(t)$  of the band pass filter can be expressed as

$$r(t) = s(t) + n(t) \quad (\text{E.1-1})$$

where

$$s(t) = x(t) \sin \omega_0 t - y(t) \cos \omega_0 t \quad (\text{E.1-2})$$

and

$$n(t) = n_s(t) \sin \omega_0 t - n_c(t) \cos \omega_0 t \quad (\text{E.1-3})$$

In equation (E.1-2) and (E.1-3)  $\omega_0$  is the center frequency of the pass band,  $x(t)$  and  $y(t)$  are slowly time varying function which can be either deterministic or random in nature,  $n_s(t)$  and  $n_c(t)$  are slowly time varying random processes.

The input to the quadratic detector can be expressed as

$$r(t) = (x(t) + n_s(t)) \sin \omega_0 t - (y(t) + n_c(t)) \cos \omega_0 t \quad (\text{E.1-4})$$

$$\begin{aligned} &= \left[ (x(t) + n_s(t))^2 + (y(t) + n_c(t))^2 \right]^{1/2} \sin(\omega_0 t - \theta) \\ &= e(t) \sin(\omega_0 t - \theta) \end{aligned} \quad (\text{E.1-5})$$

where

$$\theta = \tan^{-1} \left( \frac{y(t) + n_c(t)}{x(t) + n_s(t)} \right) \quad (\text{E.1-6})$$

$$e(t) = \left[ (x(t) + n_s(t))^2 + (y(t) + n_c(t))^2 \right]^{1/2} \quad (\text{E.1-7})$$

The output of the quadratic detector is the square of the input envelope so

$$\begin{aligned} z(t) = e(t)^2 &= (x(t) + n_s(t))^2 + (y(t) + n_c(t))^2 \\ &= (x^2(t) + y^2(t)) + (n_s^2(t) + n_c^2(t)) + 2x(t)n_s(t) + 2y(t)n_c(t) \end{aligned} \quad (\text{E.1-8})$$

The sample and average processes following the quadratic detector can be expressed by:

$$Q = \frac{1}{N} \sum_{i=1}^N z(t_i) \quad (\text{E.1-9})$$

## E.2.0 PROBABILITY DISTRIBUTION WHEN SIGNAL IS PRESENT

In the following analysis the signal  $s(t)$  in equation (E.1-1) and (E.1-2) are assumed to be deterministic.

### E.2.1 Probability Distribution of the Noise $n(t)$

For this analysis a narrow band Gaussian random process is assumed for the noise  $n(t)$ . A zero mean is also assumed with variance  $\frac{2}{n}$ . It follows that  $n_s(t)$  and  $n_c(t)$  are also zero mean Gaussian random processes with the same variance

$\frac{2}{n}$ . (For representation of narrow band Gaussian random processes see Gardner: phaselock techniques.)

### E.2.2 Probability Distribution of $e(t)$ ; the Envelope of $r(t)$

The envelope  $e(t)$  of the quadratic detector input  $r(t)$  can be expressed as

$$e(t) = \left[ (x(t) + n_s(t))^2 + (y(t) + n_c(t))^2 \right]^{1/2} \quad (\text{E.2-1})$$

let

$$\begin{cases} \alpha(t) = x(t) + n_s(t) \\ \beta(t) = y(t) + n_c(t) \end{cases} \quad (\text{E.2-2})$$

then

$$e(t) = (\alpha^2(t) + \beta^2(t))^{1/2} \quad (\text{E.2-3})$$

It follows that  $\alpha(t), \beta(t)$  are still Gaussian random variables with variance  $\sigma_n^2$  and mean  $x(t)$  and  $y(t)$ , respectively.

Since  $n_c(t), n_s(t)$  are statistically independent, it follows that  $\alpha(t), \beta(t)$  are statistically independent and their joint probability density function is

$$f_{\alpha\beta}(\alpha, \beta) = \frac{1}{2\pi\sigma_n^2} e^{-\frac{(\alpha-x)^2 + (\beta-y)^2}{2\sigma_n^2}} \quad (\text{E.2-4})$$

The probability density function of

$$e(t) = (\alpha^2(t) + \beta^2(t))^{1/2}$$

can be found via the transformation

$$\begin{cases} \alpha = e \cos \theta \\ \beta = e \sin \theta \end{cases}$$

It follows that

$$f_e(e) de = \iint_{\Delta D_e} f_{\alpha\beta}(\alpha, \beta) d\alpha d\beta = \frac{1}{2\pi\sigma_n^2} \int_0^{2\pi} e^{-\frac{(e\cos\theta - x)^2 + (e\sin\theta - y)^2}{2\sigma_n^2}} e de d\theta$$

$$\therefore f_e(e(t)) = \frac{e(t)}{\sigma_n^2} \cdot \exp\left[-(e^2(t) + x^2(t) + y^2(t))/(2\sigma_n^2)\right] \cdot I_0\left(\frac{e(t) \sqrt{x^2(t) + y^2(t)}}{\sigma_n^2}\right), e(t) > 0$$

(E.2-5)

Where  $I_0(\cdot)$  is the modified Bessel function of order zero,

$f_e(\cdot)$  is the probability density function of the envelope  $e(t)$ .

### E.2.3 Probability Distribution of $q(t)$ ; the Quadratic Detector Output

The quadratic detector output  $q(t)$  is related to the envelope  $e(t)$  of its input and can be expressed as

$$q(t) = e^2(t) \tag{E.2-6}$$

The probability density function of  $q(t)$  can be found from that of  $e(t)$  to be

$$\begin{aligned} f_q(q(t)) &= \frac{1}{2\sqrt{q(t)}} \cdot f_e(\sqrt{q(t)}) \\ &= \frac{1}{2\sigma_n^2} \exp\left[-(q(t) + x^2(t) + y^2(t))/(2\sigma_n^2)\right] \cdot I_0\left(\frac{\sqrt{q(t)} \cdot \sqrt{x^2(t) + y^2(t)}}{\sigma_n^2}\right), q(t) > 0 \end{aligned}$$

(E.2-7)

#### E.2.4 Probability Distribution of the Sample Average Q(t)

$$\begin{aligned}
 Q &= \frac{1}{N} (f(t_1) + f(t_2) + \dots + f(t_N)) \\
 &= \frac{1}{N} (e^2(t_1) + e^2(t_2) + \dots + e^2(t_N)) \\
 &= \frac{1}{N} (\alpha^2(t_1) + \alpha^2(t_2) + \dots + \alpha^2(t_N) + \beta^2(t_1) + \beta^2(t_2) + \dots + \beta^2(t_N)) \\
 &= (\alpha(t_1)/\sqrt{N})^2 + (\alpha(t_2)/\sqrt{N})^2 + \dots + (\alpha(t_N)/\sqrt{N})^2 + (\beta(t_1)/\sqrt{N})^2 + (\beta(t_2)/\sqrt{N})^2 + \dots + (\beta(t_N)/\sqrt{N})^2 \\
 &= X_1^2 + X_2^2 + \dots + X_N^2 + X_{N+1}^2 + \dots + X_{2N}^2 \quad (E.2-8)
 \end{aligned}$$

$f(t_1), f(t_2), \dots, f(t_N)$  are statistically independent samples

Where  $X_i$ ,  $1 \leq i \leq N$  } is normally distributed with mean  $\alpha(t_i)/\sqrt{N}$  and variance  $\sigma_n^2/N$

$N+1 \leq i \leq 2N$  } is normally distributed with mean  $\beta(t_i)/\sqrt{N}$  and variance  $\sigma_n^2/N$

Define

$$W = \frac{Q}{\sigma_n^2/N} = \sum_{i=1}^{2N} \left( \frac{X_i}{\sigma_n/N} \right)^2 = \sum_{i=1}^{2N} Y_i^2 \quad (E.2-9)$$

**REPRODUCIBILITY OF THE  
ORIGINAL PAGE IS POOR**

Each  $Y_i, 1 \leq i \leq N$

normally distributed with mean  $x(t_i)/(\sigma_n/\sqrt{N})$  and unity variance.

$N+1 \leq i \leq 2N$

normally distributed with mean  $y(t_i)/(\sigma_n/\sqrt{N})$  and unity variance.

It follows that  $W$  has a noncentral  $\chi^2$  distribution with  $2N$  degree freedom and a noncentral parameter

$$\lambda = \sum_{i=1}^N \left[ \left( \frac{x(t_i)}{\sigma_n/\sqrt{N}} \right)^2 + \left( \frac{y(t_i)}{\sigma_n/\sqrt{N}} \right)^2 \right] \quad (\text{E.2-10})$$

The noncentral  $\chi^2$  density function is given by

$$f_W(W) = \frac{1}{2} \left( \frac{W}{\lambda} \right)^{N-1/2} \exp\left(-\frac{\lambda}{2} - \frac{W}{2}\right) I_{N-1}(\sqrt{W\lambda}) \quad (\text{E.2-11})$$

The mean and variance of  $W$  are easily shown to be

$$\begin{aligned} E\{W\} &= \lambda + 2N \\ V\{W\} &= 4\lambda + 4N \end{aligned} \quad (\text{E.2-12})$$

The density function of  $Q$  can be derived

$$\begin{aligned} f_Q(Q) &= \frac{N}{\sigma_n^2} f_W\left(\frac{NQ}{\sigma_n^2}\right) \\ &= \frac{N}{2\sigma_n^2} \left( \frac{N/\sigma_n^2 \cdot Q}{\lambda} \right)^{N-1/2} \exp\left(-\frac{\lambda}{2} - \frac{NQ}{2\sigma_n^2}\right) I_{N-1}\left(\sqrt{\frac{N\lambda Q}{\sigma_n^2}}\right) \end{aligned} \quad (\text{E.2-13})$$

The mean and variance of  $Q$  are easily shown to be

$$\begin{aligned} E\{Q\} &= \frac{\sigma_n^2}{N} (\lambda + 2N) \\ V\{Q\} &= \left(\frac{\sigma_n^2}{N}\right)^2 (4\lambda + 4N) \end{aligned} \quad (\text{E.2-14})$$

For discussion of noncentral  $\chi^2$  distribution refer to Whalen "Detection of Signals in Noise" Academic Press, 1971).

### I.3.0 PROBABILITY DISTRIBUTION WITH ABSENCE OF SIGNAL

#### I.3.1 Probability Distribution of the Noise $n(t)$

For this analysis a narrow band Gaussian random process is assumed for the noise  $n(t)$ . A zero mean is also assumed with variance  $\sigma_n^2$ . It follows that  $n_s(t)$  and  $n_c(t)$  are also zero mean Gaussian random processes with the same variance  $\sigma_n^2$ . (For representation of narrow band Gaussian random processes see Gardner: phaselock techniques.)

#### I.3.2 Probability Distribution of $e(t)$

Set  $x(t)=y(t)=0$  in equation (E.2-5). We have the probability density function for the no signal case

$$f_e(e(t)) = \frac{1}{\sigma_n^2} \exp(-e^2(t)/(2\sigma_n^2)) \quad (\text{E.2-15})$$

#### I.3.3 Probability Distribution of $q(t)$

Set  $x(t)=y(t)=0$  in equation (E.2-7). We get the probability density function for the no signal case

$$f_q(q(t)) = \frac{1}{2\sigma_n^2} \exp(-q^2(t)/(2\sigma_n^2)) \quad q(t) > 0 \quad (\text{E.2-16})$$



### I.3.4 Probability Distribution of the Q

$$z(t) = e(t)^2 = n_s^2(t) + n_c^2(t)$$

$$Q = \frac{1}{N} \sum_{i=1}^N [n_s^2(t_i) + n_c^2(t_i)]$$

$$\text{let } Z = \frac{NQ}{\sigma_n^2}$$

It is clear that  $Z$  is  $\chi^2$ -distributed with  $2N$  degrees of freedom with probability density function

$$f_Z(Z) = \frac{1}{2^N \Gamma(N)} Z^{N-1} \cdot e^{-Z/2}, \quad Z \geq 0$$

The density function of  $Q$  can be found to be

$$f_Q(Q) = \frac{N}{\sigma_n^2} \cdot \frac{1}{2^N \Gamma(N)} \left( \frac{NQ}{\sigma_n^2} \right)^{N-1} \cdot e^{-NQ/(2\sigma_n^2)}, \quad Q \geq 0 \quad (\text{E.2-17})$$

### I.4.0 PHYSICAL MEANING OF THE QUANTITY Q

It is interesting to see the mean value of the detector output

$$\begin{aligned} E\{Q\} &= E\{e^2\} = E\{(x(t) + n_s(t))^2 + (y(t) + n_c(t))^2\} \\ &= E\{x^2(t) + y^2(t)\} + E\{n_s^2(t) + n_c^2(t)\} + 2E\{x(t)\}E\{n_s(t)\} + 2E\{y(t)\}E\{n_c(t)\} \\ &= E\{x^2(t) + y^2(t)\} + E\{n_s^2(t) + n_c^2(t)\} \end{aligned} \quad (\text{E.2-18})$$

or

$$E\{x^2(t) + y^2(t)\} = E\{Q\} - E\{n_s^2(t) + n_c^2(t)\} \quad (\text{E.2-19})$$

The quantity  $E\{x^2(t) + y^2(t)\}$  is the average signal power.  
and  $E\{n_s^2(t) + n_c^2(t)\}$  is the average noise power.

Equation (E.2-18) or (E.2-19) actually implies that the average signal power is equal to the average detector output minus the average noise power.

So if the average detector output and the average noise power are known then the average signal power can be computed by equation (E.2-19). Unfortunately, the true average of the detector output and the noise power are not available in practice. Sample mean are used instead of the true mean value. So at the output of the detector a sample and average circuit is used to take the sample average of the detector output with signal present and with signal absent. The difference gives an estimate of the average signal power. The reliability of the answer depends on the number of samples used.

The average power estimates can be implemented by two identical circuits of the type shown in Figure E-2 connected as follows:

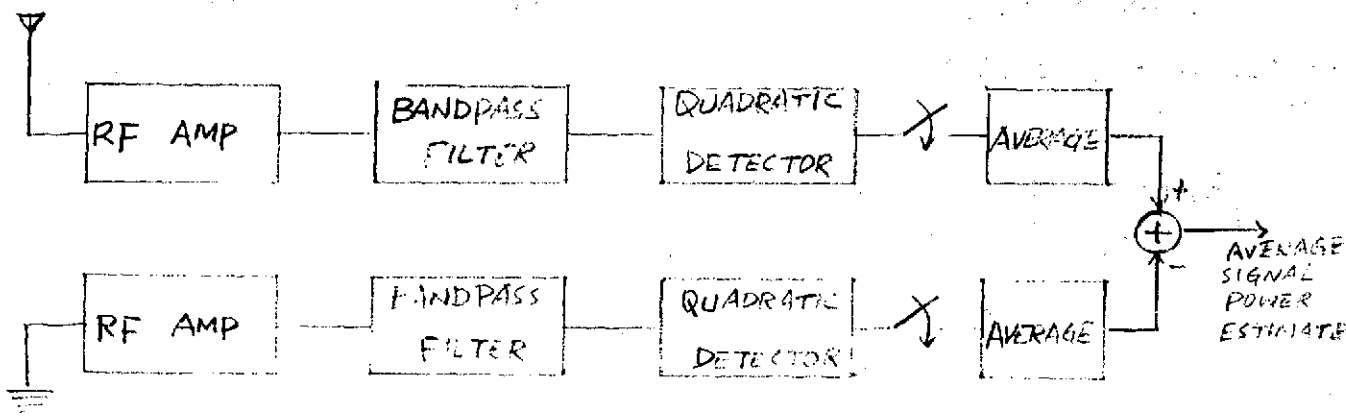


FIGURE E-2 AVERAGE SIGNAL POWER ESTIMATOR

## E SIGNAL POWER DETECTION

### II. PEAK SIGNAL POWER DETECTION

#### E2.1.0 INTRODUCTION

In RFI measurement, sometimes peak power level during a time interval is a desirable quantity in addition to the average power in the same interval. Another quantity may be of value to some type of users in the average peak power expected in an arbitrary fixed time interval. For example, a particular user operates in 1000  $\mu$ sec interval. He may be interested in the expected peak power level in 1000  $\mu$ sec span. This type of peak power detection problem will be discussed in the next few sections. Two models will be discussed in the following.

#### E2.2.0 MODELS

##### E2.2.1 Model I

The model for the peak power detection problem is illustrated in Figure E2-1 below.

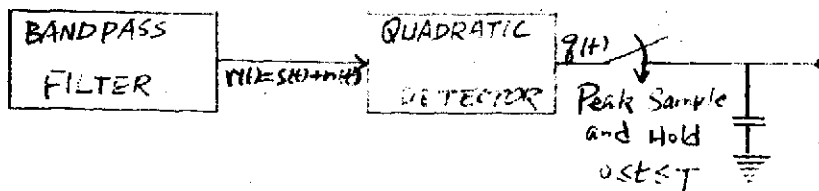


FIGURE E2-1

The quantity  $s(t)$ ,  $n(t)$ ,  $r(t)$  and  $q(t)$  has the same characteristics as that of the average power detection case and will not be repeated here refer to Section I, paragraphs E.1.0 to E.2.3

The peak sample and hold circuit following the quadratic detector can be implemented in either analog or digital fashions. The analog way is easy to implement physically, but difficult to analyze. The digital method is somewhat easier to analyze and implement. It can be implemented by sampling at the output of the quadratic detector for  $N$  independent samples then find the maximum. The meaning of the maximum will be discussed later.

#### E2.3.0 PROBABILITY DISTRIBUTION OF THE MAX OF N INDEPENDENT RANDOM VARIABLES

Let's consider two random variables  $x$  and  $y$  ( $x$  and  $y$  may be statistically dependent). Form a new random variable

$$Z = \max(x, y) \quad (E2.3-1)$$

The region  $D_z$  such that

$\max(x, y) \leq z$  that is  $x \leq z$  and  $y \leq z$  is shown in Figure

E2-2

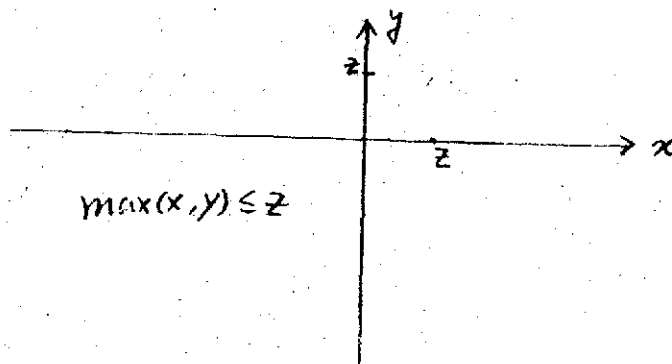


FIGURE E2-2

It is obvious that the distribution function

$$F_z(z) = F_{xy}(z, z) \quad (\text{E2.3-2})$$

The corresponding probability density function is found by differentiation of equation III-2.

$$f_z(z) = \frac{\partial F_{xy}(z, z)}{\partial x} + \frac{\partial F_{xy}(z, z)}{\partial y} = \int_{-\infty}^z f_{xy}(z, y) dy + \int_{-\infty}^z f_{xy}(x, z) dx \quad (\text{E2.3-3})$$

If  $x$  and  $y$  are statistically independent, then

$$F_z(z) = F_x(z) F_y(z) \quad (\text{E2.3-4})$$

$$f_z(z) = f_x(z) F_y(z) + f_y(z) F_x(z) \quad (\text{E2.3-5})$$

The results above can easily be extended to arbitrarily finite number of random variables.

For example  $X_1, X_2, \dots, X_N$  be  $N$  arbitrary random variables.

We form a new random variable

$$W = \text{Max}(X_1, X_2, \dots, X_N) \quad (\text{E2.3-6})$$

Then

$$F_w(w) = F_{x_1, x_2, \dots, x_N}(w, w, \dots, w) \quad (\text{E2.3-7})$$

$$f_w(w) = \frac{\partial F_{x_1, x_2, \dots, x_N}(w, w, \dots, w)}{\partial x_1} + \frac{\partial F_{x_1, x_2, \dots, x_N}(w, w, \dots, w)}{\partial x_2} + \dots + \frac{\partial F_{x_1, x_2, \dots, x_N}(w, w, \dots, w)}{\partial x_N} \quad (\text{E2.3-8})$$

If  $x_1, x_2, \dots, x_N$  are statistically independent then

$$F_w(w) = F_{x_1}(w) F_{x_2}(w) \dots F_{x_N}(w) = \prod_{i=1}^N F_{x_i}(w) \quad (\text{E2.3-9})$$

$$f_z(z) = \sum_{i=1}^N \left[ \left( \prod_{\substack{j=1 \\ j \neq i}}^N F_{x_j}(z) \right) f_{x_i}(z) \right] \quad (\text{E2.3-10})$$

#### E2.4.0 PROBABILITY DISTRIBUTION OF THE MAX OF N INDEPENDENT SAMPLES FROM THE RANDOM PROCESS $q(t)$

N independent samples are taken from the output of the quadratic detector  $q(t)$ . This corresponds to the problem of finding

$$V = \max (q(t_1), q(t_2), \dots, q(t_N)) \quad (\text{E2.3-11})$$

Where  $q(t_1), q(t_2), \dots, q(t_N)$  are identically distributed statistically random variables. The distribution of V can be found from equation (I.2-7) of Part I and equation (E2.3-10) of Part II for the signal plus noise case from equation (II.2-16) of Part I and equation (II.3-10) of Part II for the noise alone case.

#### E2.5.0 PHYSICAL MEANING OF V & U

Intuitively, the meaning of V is the peak power of the signal plus noise. The relationship between the quantity V and the peak signal power is not obvious as can be seen from the following expression.

$$\begin{aligned}
V &= \max (f(t_1), f(t_2), \dots, f(t_N)) \\
&= \max_{1 \leq i \leq N} \{f(t_i)\} \\
&= \max_{1 \leq i \leq N} \left\{ (x^2(t_i) + y^2(t_i)) + (n_c^2(t_i) + n_s^2(t_i)) + (2x(t_i)n_s(t_i) + 2y(t_i)n_c(t_i)) \right\}
\end{aligned}$$

(E2.3-12)

Under the no signal condition we use  $V_n$

$$V_n = \max_{1 \leq i \leq N} \{ (n_c^2(t_i) + n_s^2(t_i)) \}$$

(E2.3-13)

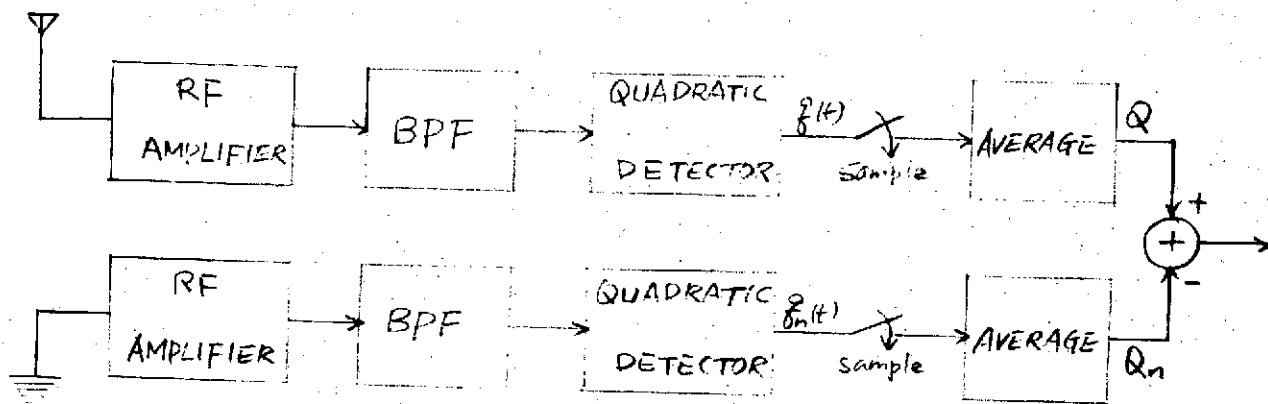
The quantity of interest is  $\max_{1 \leq i \leq N} \{ (x^2(t_i) + y^2(t_i)) \}$ .

Unfortunately, the values of  $V$  and  $V_n$  are not sufficient to

tell us about  $\max_{1 \leq i \leq N} \{ (x^2(t_i) + y^2(t_i)) \}$ . The main difficulty is the cross product term  $x(t)n_s(t) + y(t)n_c(t)$ .

## Average Signal Power Estimation Versus Peak Signal Power Estimation

### 1. Simplified Block Diagrams



<u>Signal Present</u>	<u>Signal Absent</u>
$V(t) = S(t) + n(t)$	$V_n(t) = V'(t)$
$S(t) = x(t)\sin\omega_0 t - y(t)\cos\omega_0 t$	$n'(t) = n_s'(t)\sin\omega_0 t - n_c'(t)\cos\omega_0 t$
$n(t) = n_s(t)\sin\omega_0 t - n_c(t)\cos\omega_0 t$	$g_n(t) = n_s'^2(t) + n_c'^2(t)$
$g(t) = (x(t) + n_s(t))^2 + (y(t) + n_c(t))^2$	$Q_n = \frac{1}{N} \sum_{i=1}^N g_n(t_i)$
$Q = \frac{1}{N} \sum_{i=1}^N g(t_i)$	

$$E\{g(t)\} = E\{x^2(t) + y^2(t) + n_s^2(t) + n_c^2(t) + 2x(t)n_s(t) + 2y(t)n_c(t)\}$$

$$= E\{x^2(t) + y^2(t)\} + E\{n_s^2(t) + n_c^2(t)\}$$

$$Q \approx E\{g(t)\}$$

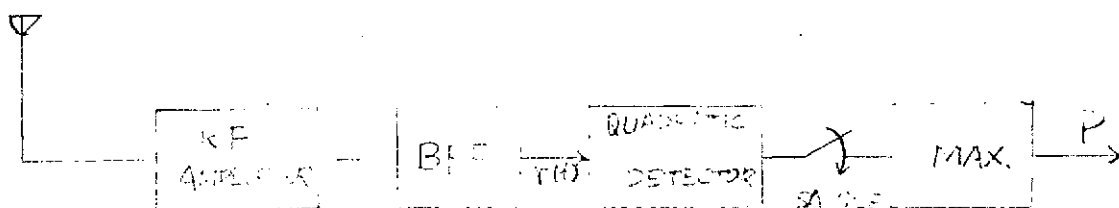
$$Q_n \approx E\{n_s^2(t) + n_c^2(t)\} = \text{Average Noise Power}$$

$$\therefore E\{x^2(t) + y^2(t)\} = E\{g(t)\} - E\{n_s^2(t) + n_c^2(t)\} = \text{Average Signal Power}$$

Average Signal Power Estimator

$$\approx Q - Q_n$$





$$r(t) = s(t) + n(t)$$

$$s(t) = x(t) \sin \omega_c t - y(t) \cos \omega_c t$$

$$n(t) = n_s(t) \sin \omega_c t - n_c(t) \cos \omega_c t$$

$$z(t) = (x(t) + n_s(t))^2 + (y(t) + n_c(t))^2$$

$$P = \max_{1 \leq i \leq N} \{z(t_i)\} = \max_{1 \leq i \leq N} \left\{ x^2(t_i) + y^2(t_i) + n_s^2(t_i) + n_c^2(t_i) + 2x(t_i)n_s(t_i) + 2y(t_i)n_c(t_i) \right\}$$

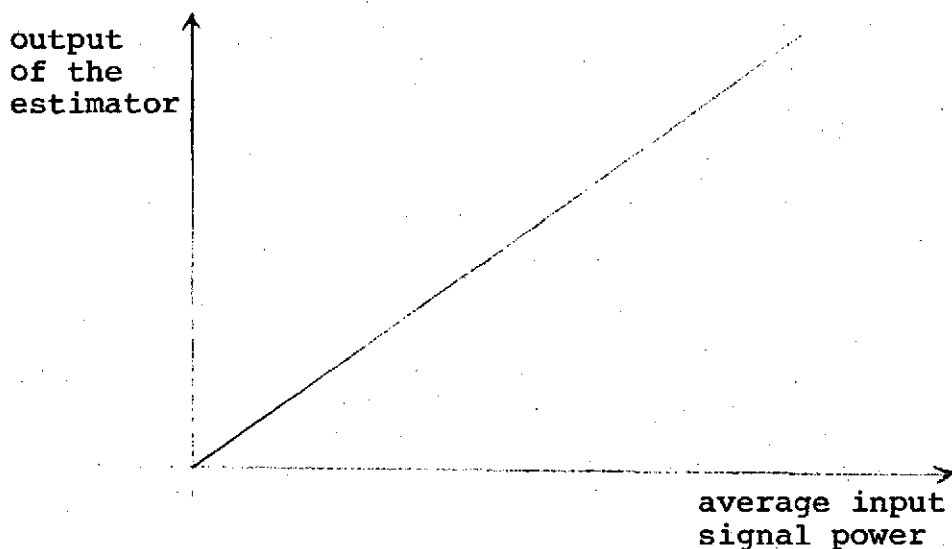
$$\approx \max_{1 \leq i \leq N} \{x^2(t_i) + y^2(t_i)\} \quad \text{for} \quad x^2(t) + y^2(t) \gg n_s^2(t) + n_c^2(t)$$

Peak Signal Power Estimator

REPRODUCIBILITY OF THE  
ORIGINAL PAGE IS POOR

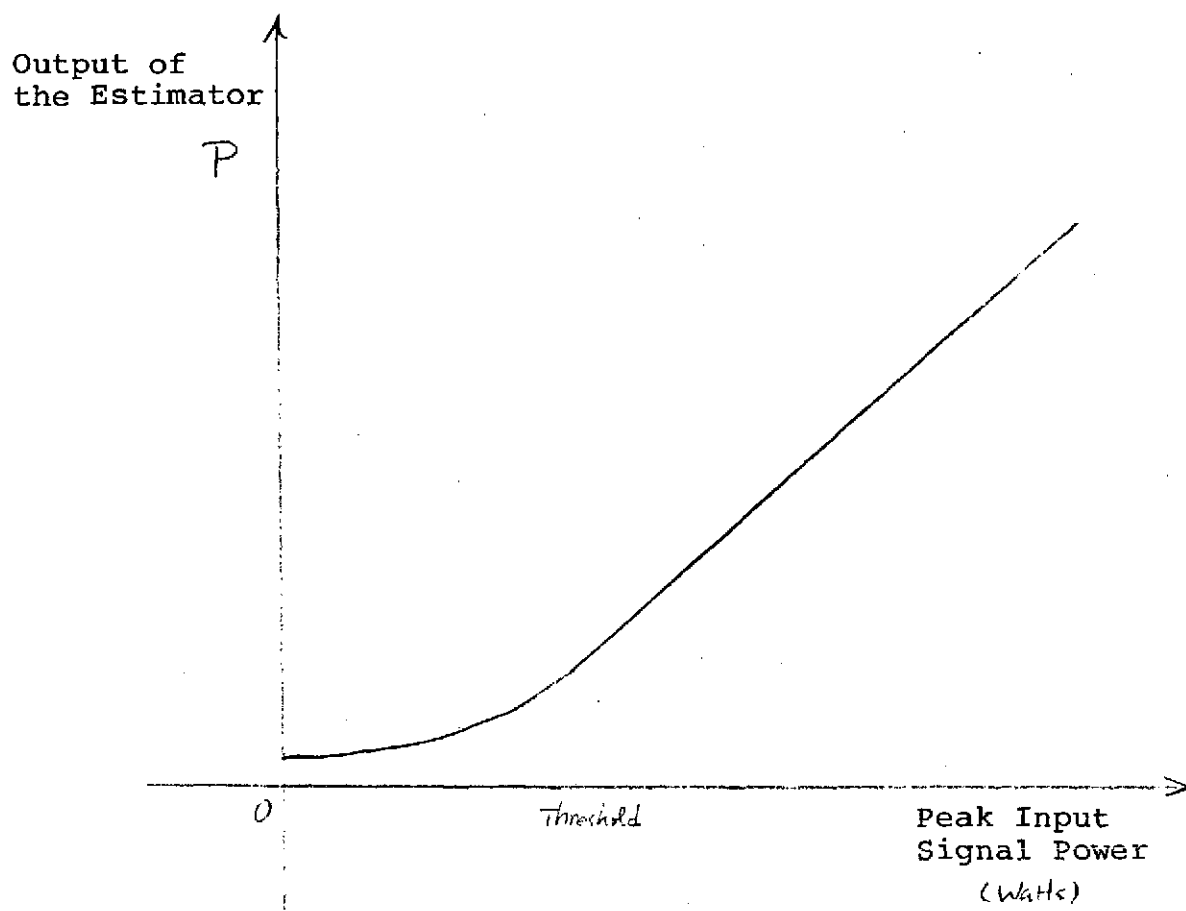
## 2. Comparison of Average and Peak Power Estimator

Average power estimator gives an estimate of the average input signal power for all signal levels within the dynamic range of the receiver. The accuracy of the estimate can be improved by increasing the number of independent samples. The calibration curve has a



### Calibration Curve for Average Power Estimator

Peak power estimator gives an estimate of the peak input signal power only when the input peak signal power is above a certain threshold. The accuracy of the estimate improves with increasing signal power. Below the threshold the noise estimator and the output gives less significant estimates as peak signal level goes down. The calibration curves has a threshold associated with it.



Calibration Curve for Peak Power Estimation